University of
MICHIGAN

Final Defense

Advances in Surface Penetrating Technologies for Imaging, Detection, and Classification

Jay A. Marble

Committee: Alfred Hero (co-chair)
Andrew Yagle (co-chair)
Eric Michielssen
Mahta Moghaddam

Surface Penetrating Technologies Problem Statement

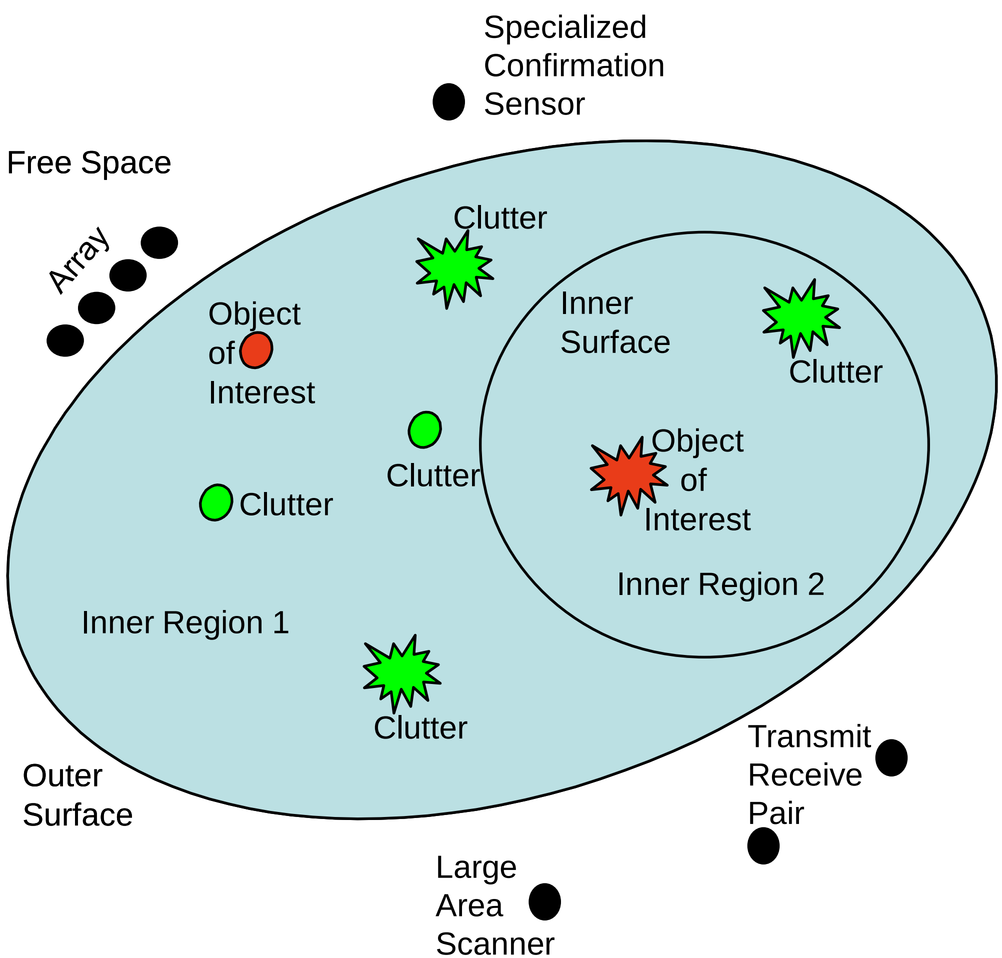

- General Problem – Objects of interest in an unknown, inhomogeneous media.
- The ultimate goal is to detect and identify the objects of interest while ignoring the clutter.
- The scope of the problem ranges from initial object imaging, to detection, to final classification.
- Classification also includes the scheduling of confirmation sensors.

Applications

- Landmine/UXO Detection
  - Ground Penetrating Radar imaging.
  - Detect and discriminate between landmines and various clutter objects.
  - Sensor scheduling of confirmation sensors.

- See-Through-Wall Radar Imaging
  - Provide authorities with accurate information concerning building interiors.
  - This can include: hidden weapons, building layouts, suspicious person tracking, methamphetamine labs.
  - Sensor scheduling for adaptive imaging.

Applications

Landmine Detection/Classification

Landmine

NOT Landmine

Discriminate between landmines and other objects using multiple sensors.

Applications
See-Through-Wall Imaging

- Problems of Interest
  - Layout Mapping of Inner Walls
  - Cache Detection
  - Suspicious Person Tracking

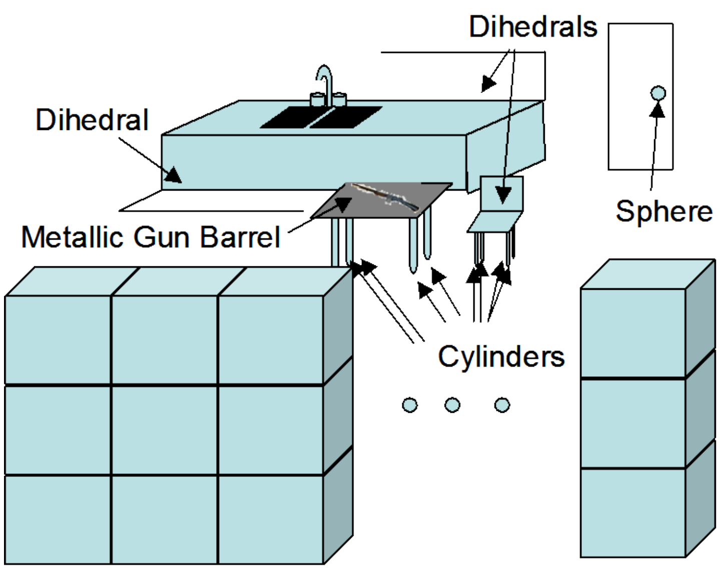

- Technical Challenges
  - Inhomogeneous Medium
    - Causes multipath scattering - ghosts
    - Unknown phase delays through wall - blurring.
  - Walls may be metal reinforced.
    - E&M Penetration difficult.
    - Requires higher frequencies, which attenuate faster.

Contribution Areas

- Non-statistical Methods
  - SNR Enhancement
  - Radar and Metal Detectors for Landmine Detection
- Statistical Methods
  - Landmine Scanning Sensors
  - Sensor Scheduling of Landmine Confirmation Sensors
- Imaging
  - Sensor Scheduling of STW Radar
  - Near Real Time STW and Landmine Radar Imaging – 2D and 3D

Non-statistical Methods
of Signal-to-Noise Ratio Enhancement

Non-statistical Methods

- SNR Enhancement of GPR Signals
  - Hyperbola Flattening Transform
  - Makes use of the un-imaged point spread function of radar echoes from landmines.
- Metal Detector Signal Processing
  - Electromagnetic Induction (EMI) Sensors
  - Utilize a dipole response model to identify basis functions.
  - Form subspace filters to enhance SNR and identify object depth and rudimentary shape.
- Vision System Methods
  - Generate a focused image of the landmine.
  - Draw a bounding box around the object to extract size and depth info.

Radar SNR Enhancement

The Hyperbola Flattening Transform

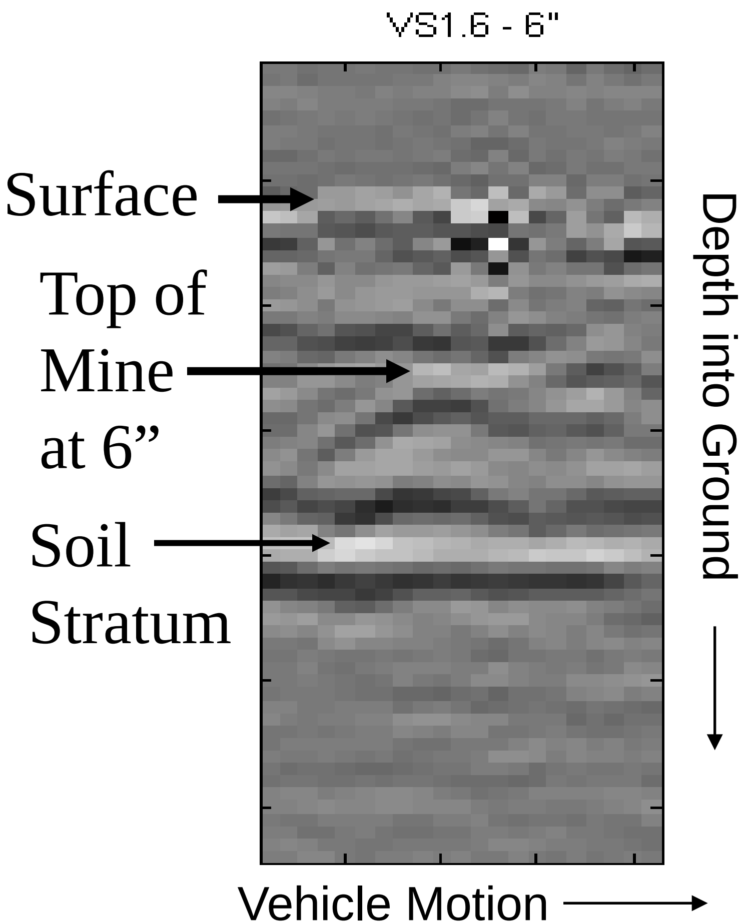

Plastic Landmine (VS1.6)

- Deeply buried plastic landmines face a low signal-to-noise ratio (SNR).
- Strata in the ground can create large radar returns that lead to false alarms.
- The Hyperbolic Flattening Transform seeks to exploit all the “energy” of the hyperbolic signature.

Radar SNR Enhancement

Hyperbola Flattening Transform

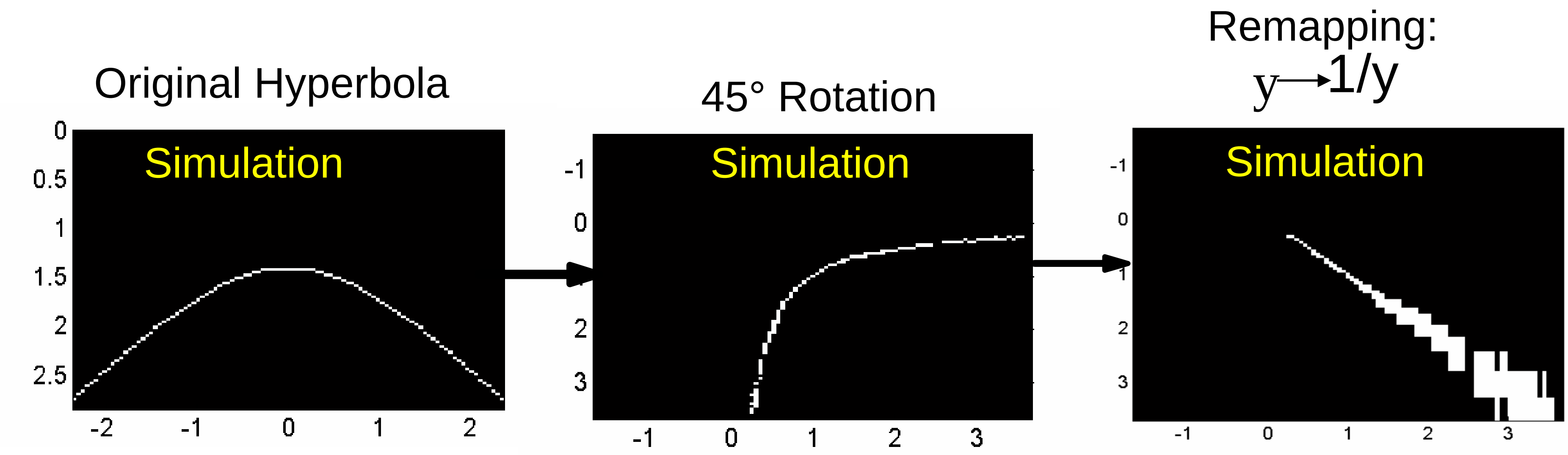

$$\frac{y^2}{d^2} - \frac{x^2}{a^2} = 1 \qquad xy = 1 \qquad \frac{x}{y} = 1$$

- The Hyperbola Flattening Transform converts a hyperbolic signature into a straight line at 45°.

Application to Simulated Data

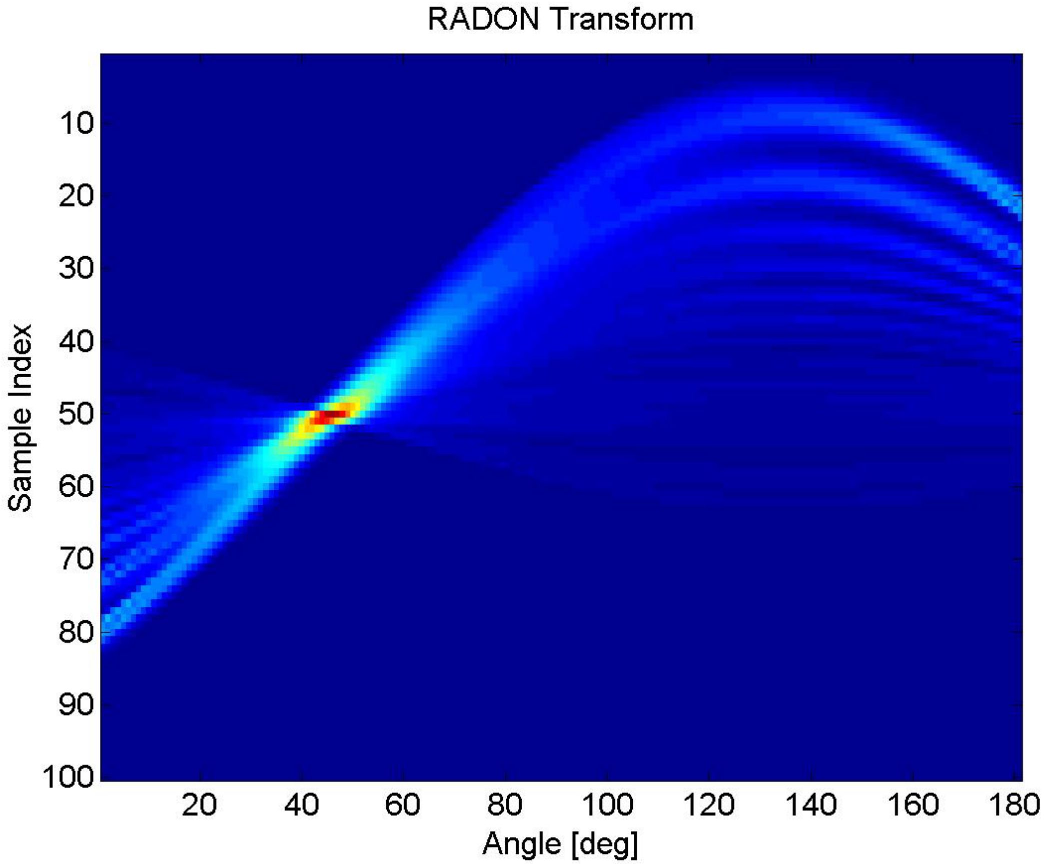

- The RADON transform creates “projections” by summing along lines.
- Projections are oriented for 0° to 180°.
- Radon Transform of the “flattened” hyperbola has a strong maximum at 45° corresponding to the “energy” contained in the hyperbola.

Application to Real Data

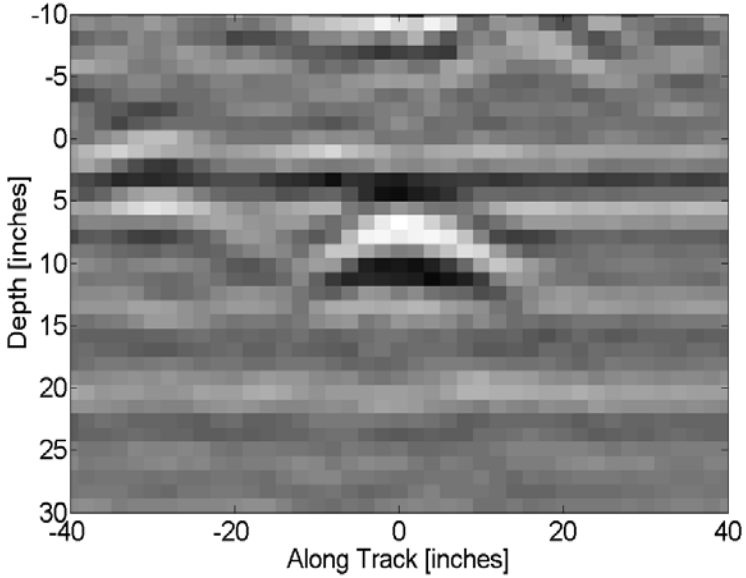

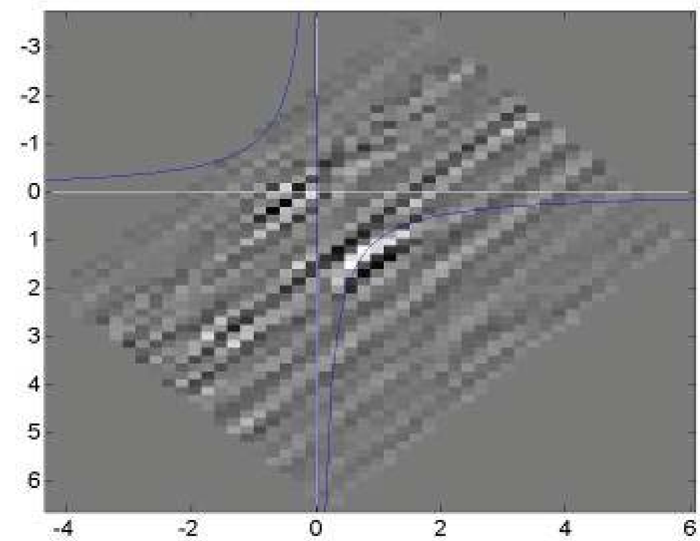

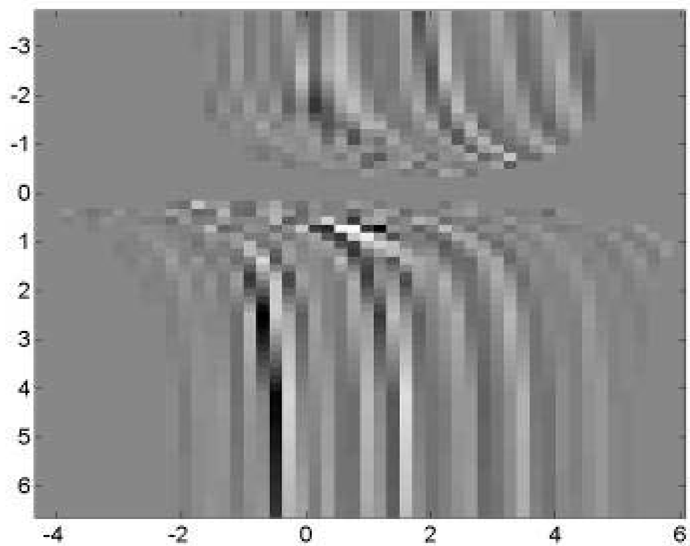

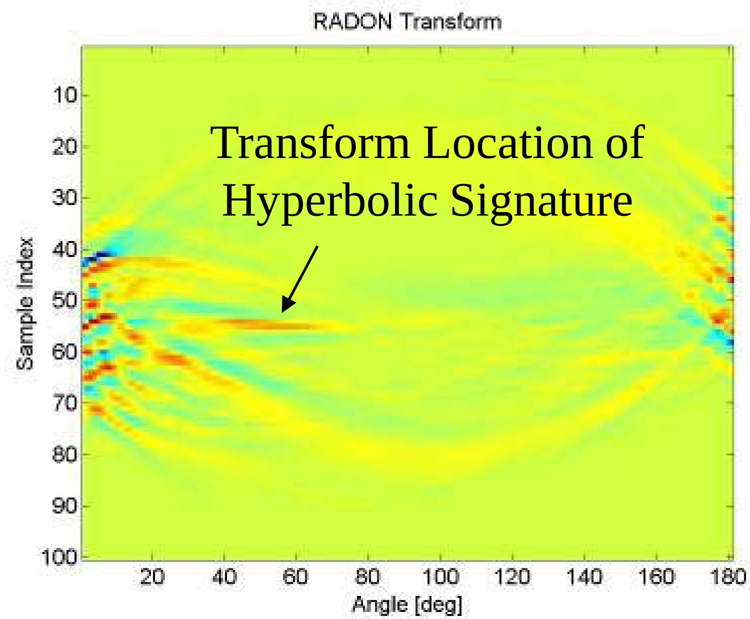

Application to Real Data

Original Image

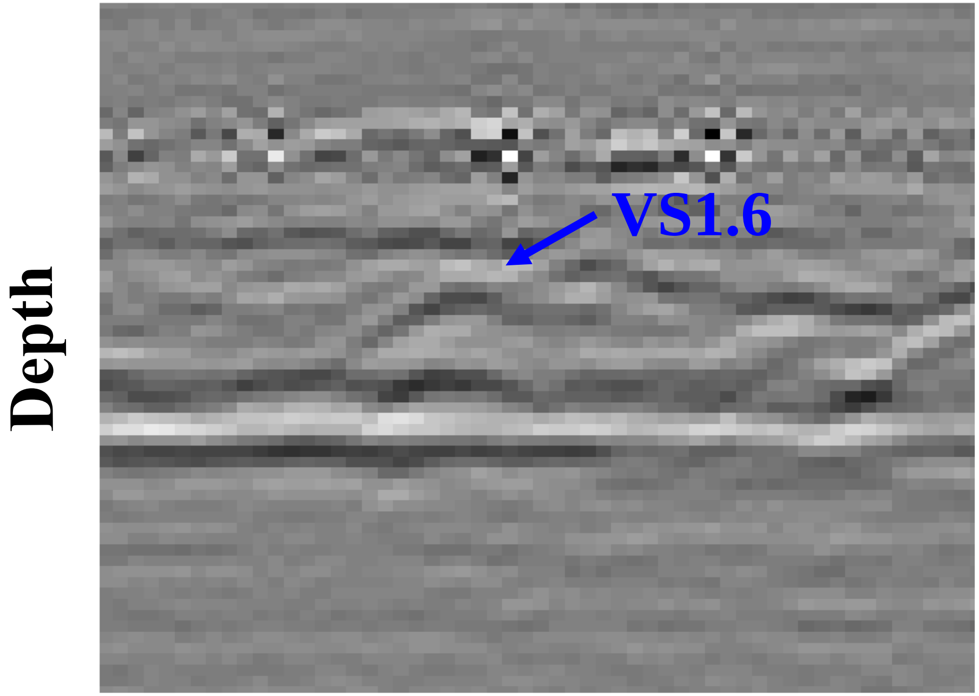

Along Track

- The HFT will now be applied as a detector.
- A small kernel is moved throughout the scene. At each location, the HFT is applied.,
- At each point the HFT is run for several values of the “a” parameter. The maximum result is placed into a detection image.

Application to Real Data

Hyperbola Detection Image

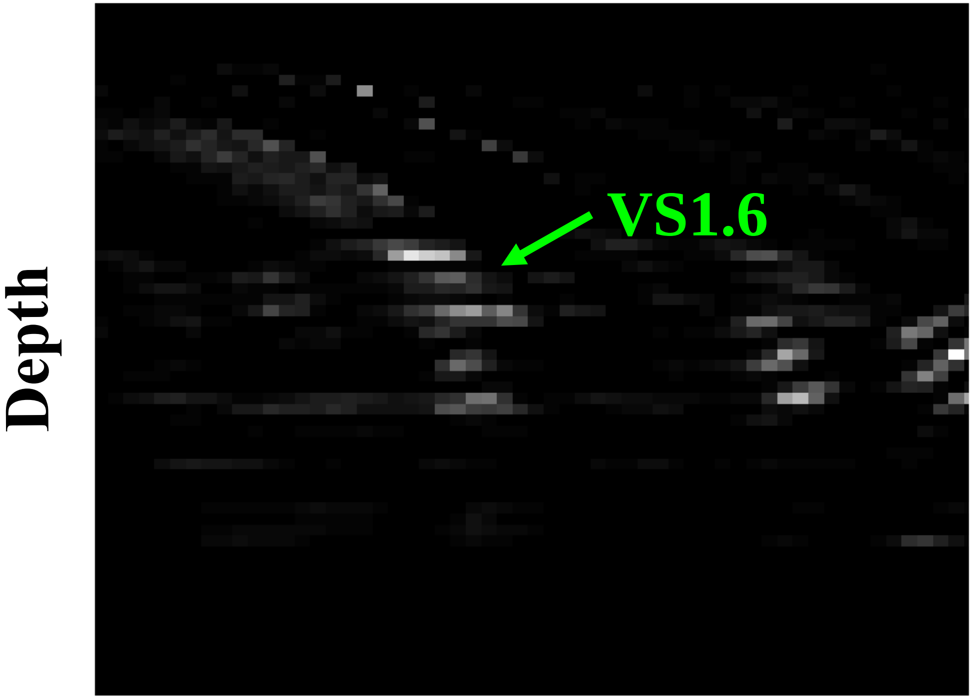

Along Track

- The HFT is applied to all locations in the scene. The detection image shown here is the result.
- Bright pixels correspond to hyperbolas. Hyperbolic signatures have been contrast enhanced, while non-hyperbolas are suppressed.

Application to Real Data

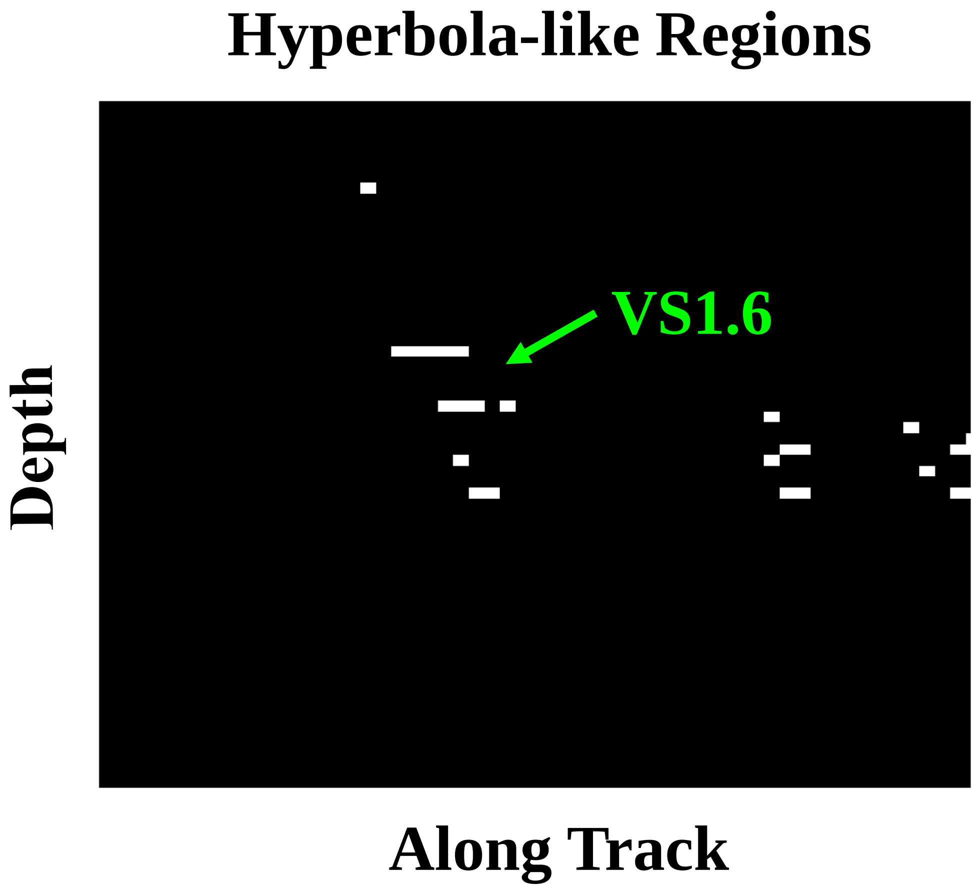

- Pixels that break a certain threshold are shown. These pixels reveal the locations of the "most hyperbola-like" signals in the scene.

- The region corresponding to the VS1.6 has been enhanced by the HFT detector.

Non-statistical Contributions

- Marble,J., Yagle,A., “The Hyperbola Flattening Transform,” SPIE: Detection and Remediation Technologies for Mines and Minelike Targets IX, April 2004, Orlando, FL.

- Marble,J., Yagle,A., “Measuring Landmine Size and Burial Depth with Ground Penetrating Radar,” SPIE: Detection and Remediation Technologies for Mines and Minelike Targets IX, April 2004, Orlando, FL.

- Marble,J.,Yagle,A., Wakefield,G, “Physics Derived Basis Pursuit in Buried Object Identification using EMI Sensors,” SPIE: Detection and Remediation Technologies for Mines and Minelike Targets X, March 2005, Orlando, FL.

Statistical Methods
of Landmine Detection and Classification

Statistical Methods

- Multimodal Landmine Detection
  - Scanning Sensor Algorithm
  - Joint Probability Densities of Two Sensors
  - Maximum A Posteriori (MAP) Detection/Classification
- Single Confirmation Sensor Scheduling
  - Information Gain Metric – Rényi Divergence
  - Deploy Sensor that Provides Greatest Information Gain
- Multiple Confirmation Sensor Scheduling
  - Collaboration with GATech and Doron Blatt
  - Develop an optimal policy for deploying multiple sensors.
  - Reinforcement learning method used for training.

Scanning Sensor Observations

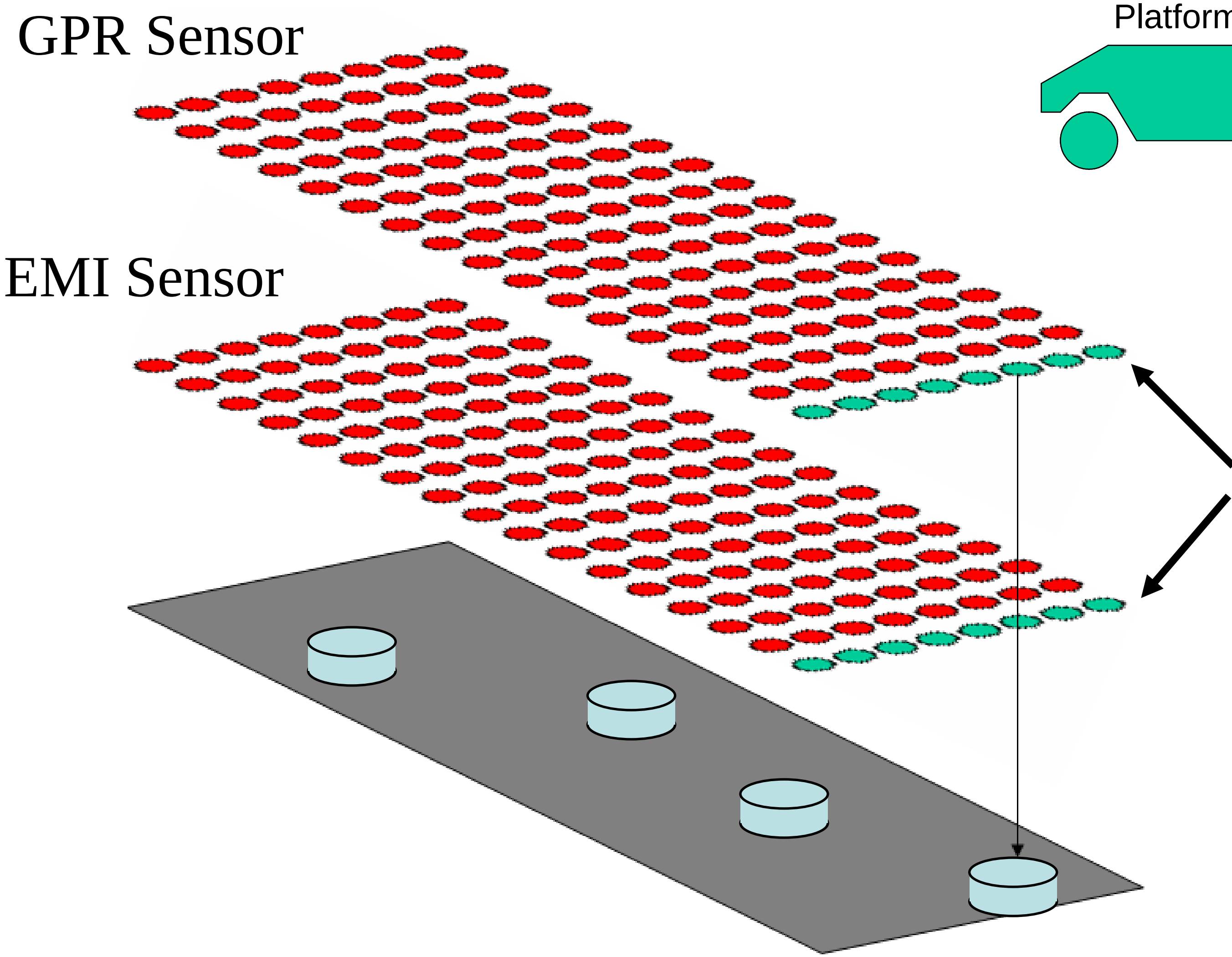

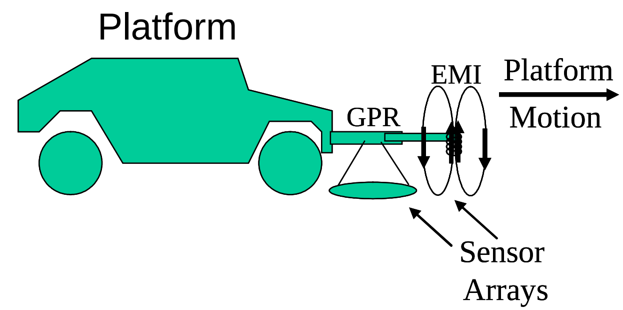

Multimodal Landmine Detection

Soil Type: Clay

Metal Landmines Only

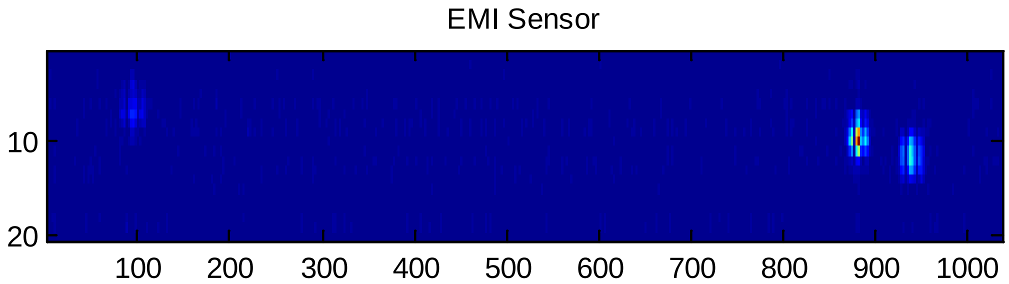

EMI Acquired “Image”

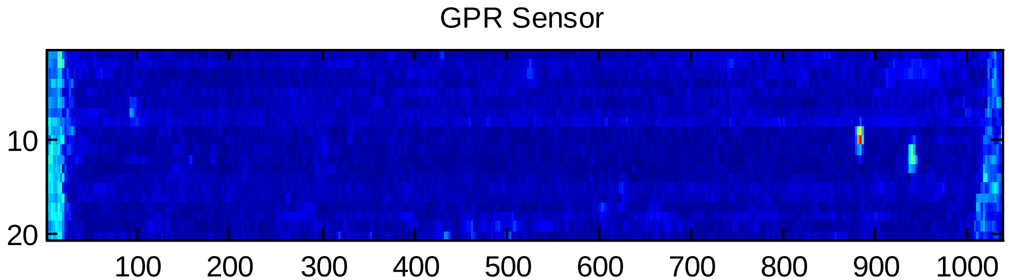

GPR Acquired “Image”

Ground Truth Markings

Simultaneous Detection and Classification

Observations

Observation Vector

$$\underline{y} = \begin{bmatrix} e \\ g \end{bmatrix}$$

Scanning Sensors

e – EMI observation

g – GPR observation

Gaussian Mixture Observation Model

$$f(\underline{y}) = \sum_{x=1}^{10} \frac{\alpha_x}{2\pi |C_x|^{\frac{1}{2}}} e^{-\frac{1}{2}(\underline{y}-\underline{\mu}_x)^T C_x^{-1}(\underline{y}-\underline{\mu}_x)}$$

2D Gaussian Model for a Given Type

$$f(\underline{y} \mid x) = \frac{1}{2\pi |C_x|^{\frac{1}{2}}} e^{-\frac{1}{2}(\underline{y}-\underline{\mu}_x)^T C_x^{-1}(\underline{y}-\underline{\mu}_x)}$$

Object Types

$$X = \{1,10\}$$

1 - background

2,3,4 - Metal AT Landmine
deep, mid-depth,
shallow

5,6,7 – Low Metal AT Landmine
deep, mid-depth, shallow

8,9,10 – Clutter Types:
aluminum, iron, and non-metal

Simultaneous Detection and Classification

> Note: This approach is the same as multiple hypothesis testing on every pixel.

- Supervised Learning
  - $$f(\underline{y} \mid x) = \frac{1}{2\pi |C_x|^{\frac{1}{2}}} e^{-\frac{1}{2}(\underline{y}-\underline{\mu}_x)^T C_x^{-1} (\underline{y}-\underline{\mu}_x)}$$
  - From available data the joint PDF of each object type is determined.
- Bayes Rule
  - $$f(x \mid \underline{y}) = \frac{f(\underline{y} \mid x) f(x)}{f(\underline{y})}$$
  - From the learned distribution we use Bayes rule to translate to the posterior distribution.
- Maximum A Posteriori Detection/Classification

$$\hat{x} = \arg\max_x [f(x \mid \underline{y})]$$

Joint Probability Densities

- Background pixel PDF shows decorrelation between EMI and GPR pixel values.
- This decorrelation makes sensor fusion very useful for false-alarm elimination.

- Metal Landmine Composite PDF
- The statistics of metal landmines are favorable for good detection performance.
- A similar PDF could be generated for plastic landmines. However, the situation is much less favorable.

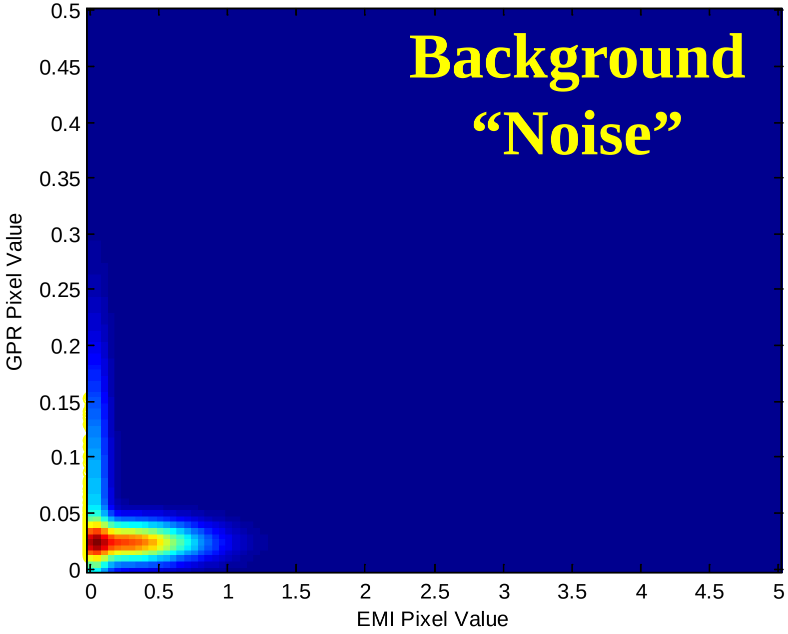

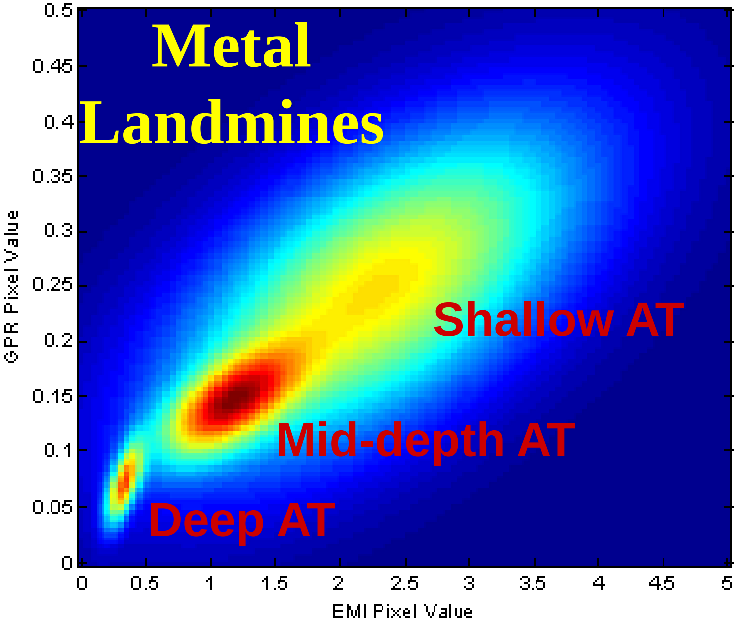

Detection Performance

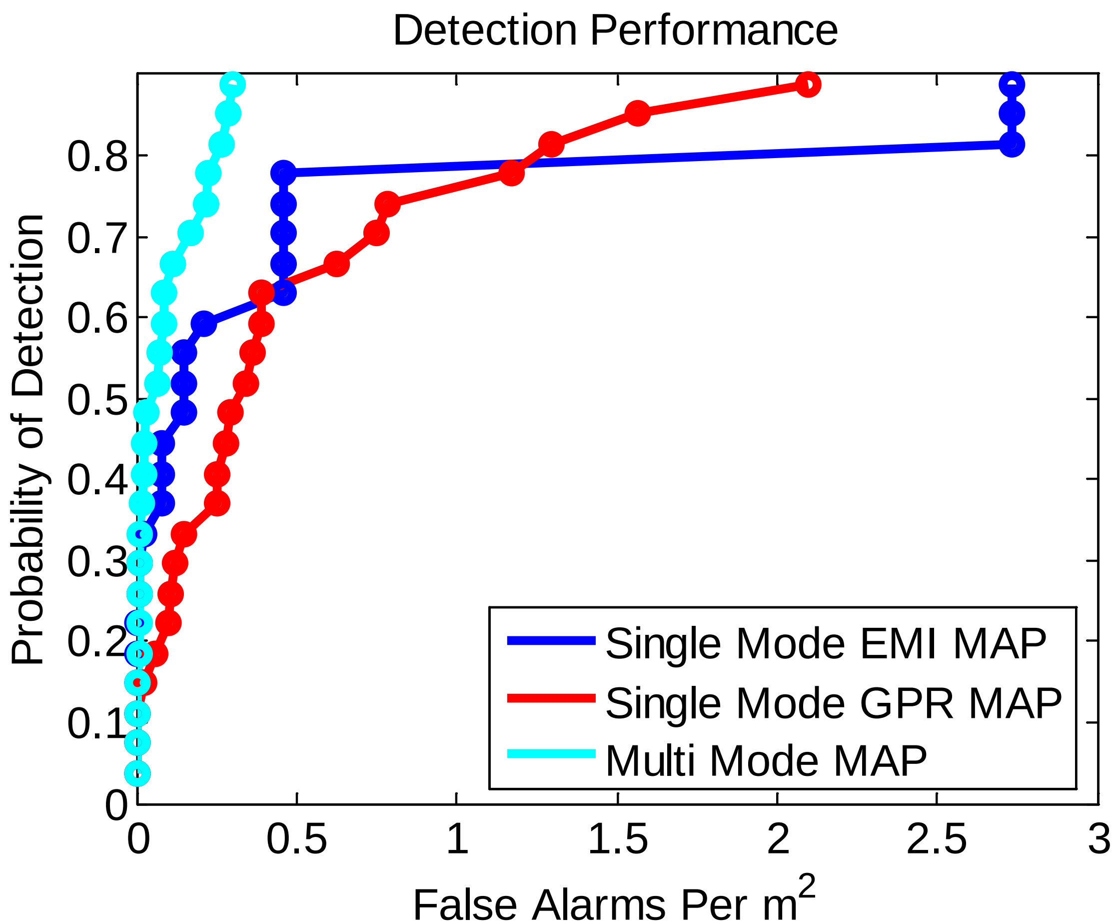

Sensor Scheduling

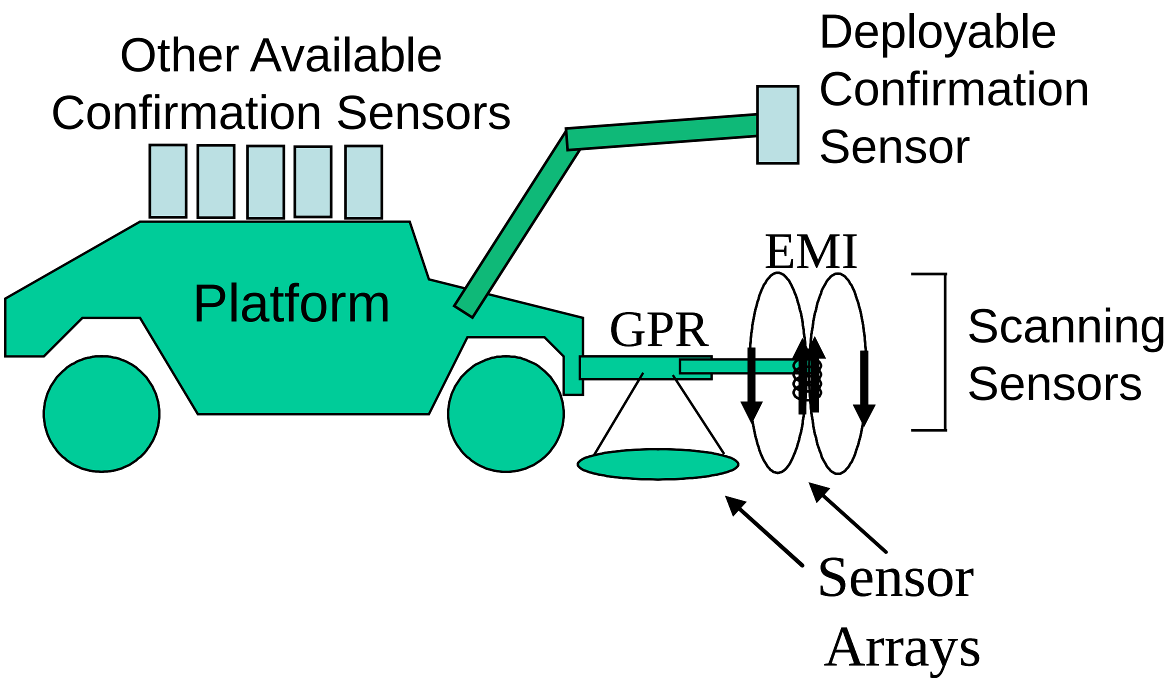

Possible Confirmation Sensors:

- E&M: Nuclear Quadrupole Resonance, Magnetometer, Broadband EMI
- Nuclear: X-ray Backscatter, Neutron Excitation
- Other: Chemical “Sniffer”, Acoustic Vibrometer, Mechanical Prodder

Sensor Scheduling Motivation

- Multiple Landmine Responses
  - Four Generic Landmine Classes:
    - Low-metal Anti-Tank
    - High-metal Anti-Tank
    - Low-metal Anti-Personnel
    - High-metal Anti-Personnel
  - Environment Impacts Response: Soil Permittivity and Conductivity
  - Object Depth Impacts Response
- Multiple Landmine Technologies
  - Non-exhaustive List: Metal Detectors, RADAR , Magnetometers, Radiometers, Seismic/Acoustic Vibrometers, Chemical Sensors, Quadrapole Resonance, Touch Probes…
  - Each sensor responds differently to landmine types and is impacted differently by depth and environment.
  - Some sensors are practical in a “scanning” context while other are only practical as “confirmation” sensors.

Scanning Sensor Simulations

- Simulated scanning sensors are used to make the scanning process realistic. It also gives experimental control over all system parameters and environmental parameters.
- Clutter objects (iron, aluminum, and non-metal) have been introduced to study false alarm rejection capabilities of algorithms.

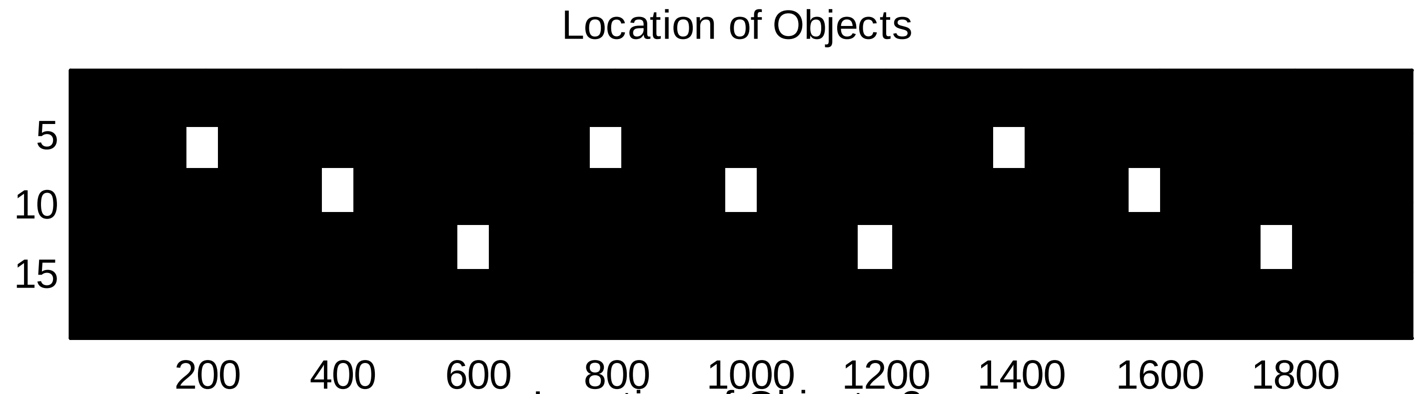

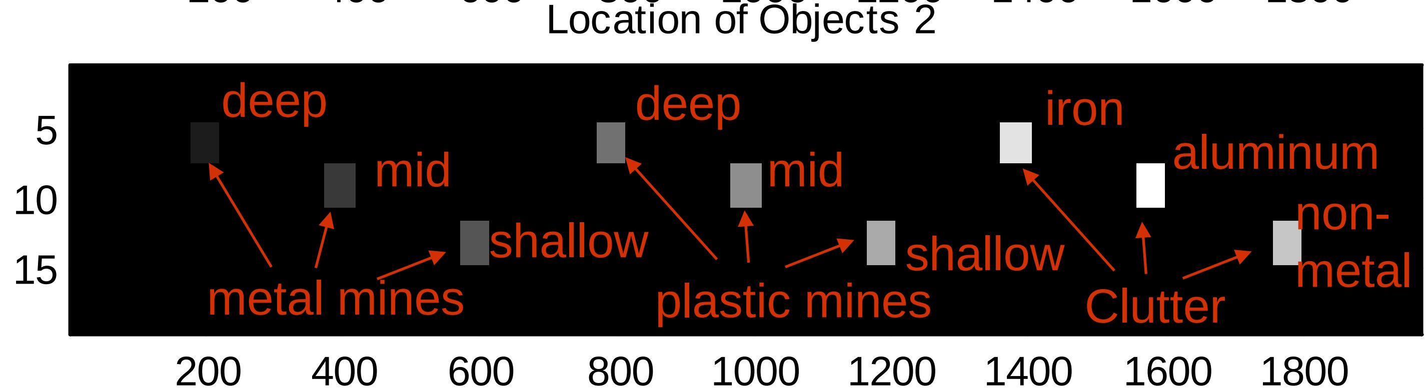

Scanning Sensor Simulations

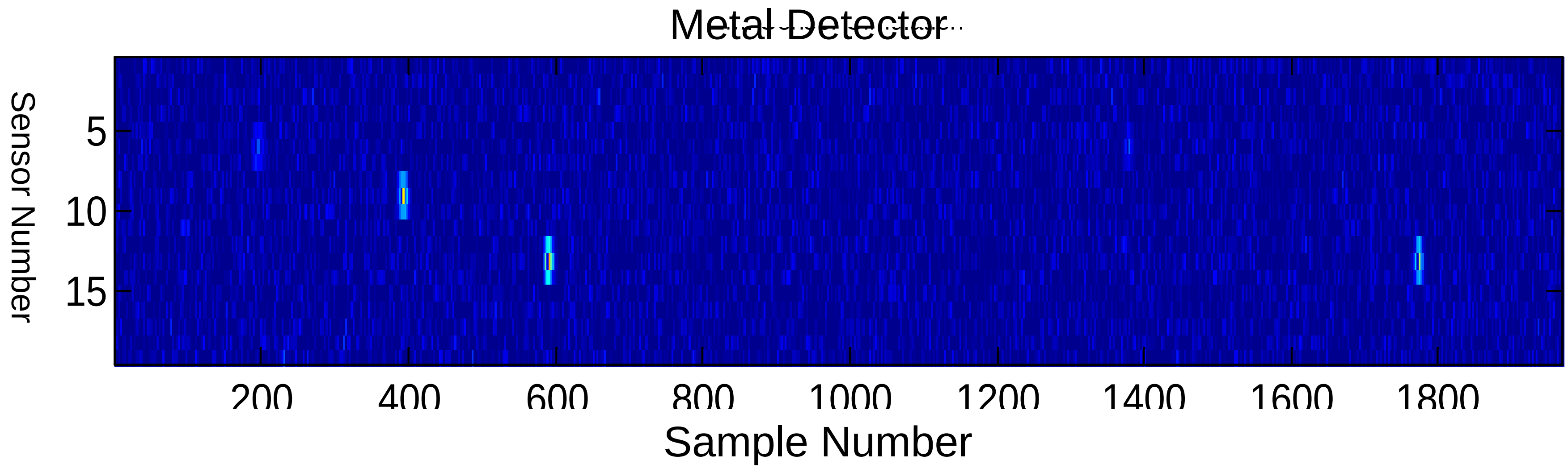

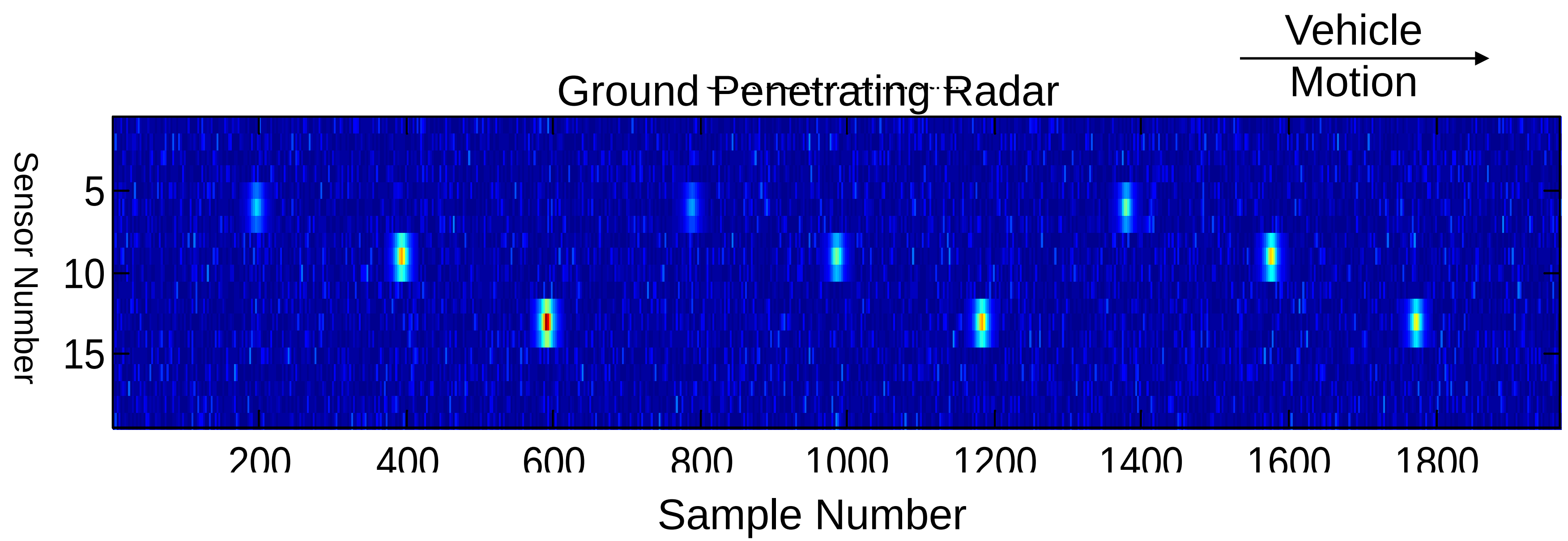

Confusion Matrix for Scanners

(MAP Detector/Classifier)

Object Types

X ={1,10}

1 - background

2,3,4 - Metal AT Landmine
deep, mid-depth, shallow

5,6,7 – Low Metal AT Landmine
deep, mid-depth, shallow

8,9,10 – Clutter Types:
aluminum, iron, and non-metal

Each Row Should Sum to One

	2	3	4	5	6	7	8	9	10
2	0.9	0	0	0	0	0	0.1	0	0
3	0	0.7	0.1	0	0	0	0	0.2	0
4	0	0.2	0.8	0	0	0	0.1	0	0
5	0	0	0	0.8	0.2	0	0	0	0
6	0	0	0	0.4	0.5	0	0	0	0.1
7	0	0	0	0.1	0.4	0.5	0	0	0
8	0.1	0.2	0	0	0	0	0.7	0	0
9	0.4	0	0	0	0	0	0	0.6	0
10	0	0	0	0	0.3	0.1	0	0	0.6

Confusion Matrix for Scanners

(MAP Detector/Classifier)

Object Types

X ={1,10}

1 - background

2,3,4 - Metal AT Landmine
deep, mid-depth, shallow

5,6,7 – Low Metal AT Landmine
deep, mid-depth, shallow

8,9,10 – Clutter Types:
aluminum, iron, and non-metal

Catastrophic Error: Missed Landmine

	2	3	4	5	6	7	8	9	10
2	0.9	0	0	0	0	0	0.1	0	0
3	0	0.7	0.1	0	0	0	0	0.2	0
4	0	0.2	0.8	0	0	0	0.1	0	0
5	0	0	0	0.8	0.2	0	0	0	0
6	0	0	0	0.4	0.5	0	0	0	0.1
7	0	0	0	0.1	0.4	0.5	0	0	0
8	0.1	0.2	0	0	0	0	0.7	0	0
9	0.4	0	0	0	0	0	0	0.6	0
10	0	0	0	0	0.3	0.1	0	0	0.6

Confusion Matrix for Scanners

(MAP Detector/Classifier)

Object Types

X ={1,10}

1 - background

2,3,4 - Metal AT Landmine
deep, mid-depth, shallow

5,6,7 – Low Metal AT Landmine
deep, mid-depth, shallow

8,9,10 – Clutter Types:
aluminum, iron, and non-metal

Undesirable Error: False Alarm

	2	3	4	5	6	7	8	9	10
2	0.9	0	0	0	0	0	0.1	0	0
3	0	0.7	0.1	0	0	0	0	0.2	0
4	0	0.2	0.8	0	0	0	0.1	0	0
5	0	0	0	0.8	0.2	0	0	0	0
6	0	0	0	0.4	0.5	0	0	0	0.1
7	0	0	0	0.1	0.4	0.5	0	0	0
8	0.1	0.2	0	0	0	0	0.7	0	0
9	0.4	0	0	0	0	0	0	0.6	0
10	0	0	0	0	0.3	0.1	0	0	0.6

Confirmation Sensor Scheduling

- Sensor Models
  - $$f(y_a \mid x) \sim \mathrm{N}\left(\mu_a, \sigma_a^2\right)$$
  - y_a is the observation to be made by deploying Sensor *a* against Object *x*.
- Performance Predictions
  - Let: $$p(x \mid a) = \frac{f(y_a \mid x)\, p(x)}{\sum_x f(y_a \mid x)}$$
  - From the sensor response distributions we use Baye's Rule to translate to the expected posterior distribution for each object type.
- Rényi Information Gain in Discrete Form

$$\hat{a} = \arg\max_a \left[\frac{1}{1-\alpha} \ln\left(\sum_x p^{\alpha}(x \mid \underline{y})\, p^{1-\alpha}(x \mid a) \right) \right]$$

Note: $\underline{y}$ implies all previously obtained observations.

Confirmation Sensor Scheduling

Confirmation Sensor Statistics Assignments

Average for Each Object Type

Action/Sensor	1	2	3	4	5	6	7	8	9	10
1	0.01	4.5	5.5	6.5	1.5	1.6	1.7	4.5	9.0	1.5
2	0	8	8	8	2	2	2	6	6	0.5
3	0.25	0.25	0.25	0.25	0.25	0.25	0.25	0.25	0.25	0.25
4	0	9	9	9	4.5	4.5	4.5	1.5	1.5	0.75
5	0.75	9	6	3	9	6	3	3	3	3
6	0	9	9	9	9	9	9	3	3	4.5

Variance for Each Object Type

Action/Sensor										
1	2	0.5	0.5	0.5	2	2	2	0.5	0.5	2
2	3	1	1	1	2	2	2	1	1	3
3	0.25	0.25	0.25	0.25	0.25	0.25	0.25	0.25	0.25	0.25
4	1.25	1.25	1.25	1.25	2.25	2.25	2.25	3.25	3.25	4.25
5	0..75	2.25	1.25	0.75	2.25	1.25	0.75	0.75	0.75	0.75
6	1.25	3.25	2.25	1.25	3.25	2.25	1.25	1.25	1.25	1.25

Confirmation Sensor Scheduling

Information Gain Metric - Rényi Divergence

$$D(f_1 \| f_0) = \frac{1}{1-a} \ln\left(\int f^{a}{}_1(x) f^{1-a}{}_0(x) dx \right)$$

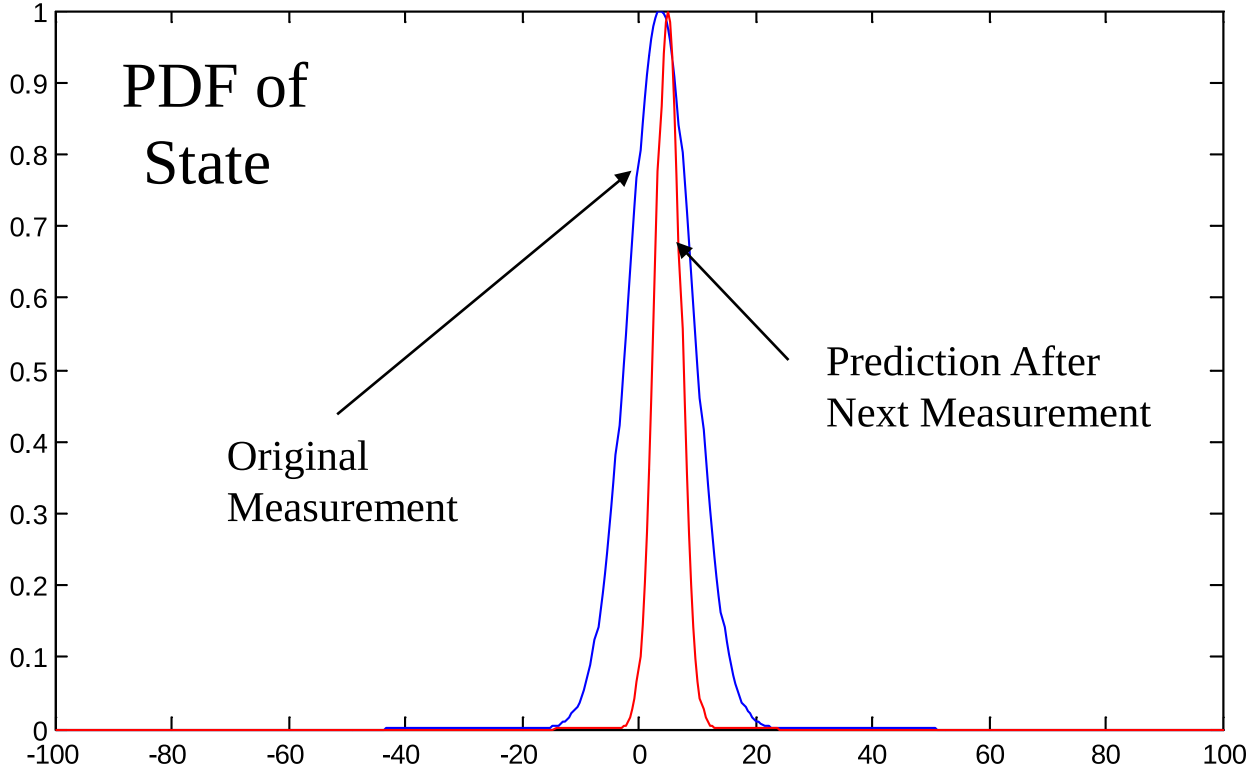

Confirmation Sensor Scheduling

Iron Clutter Object Example

EMI

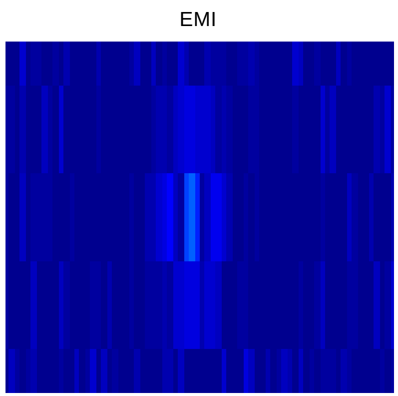

GPR

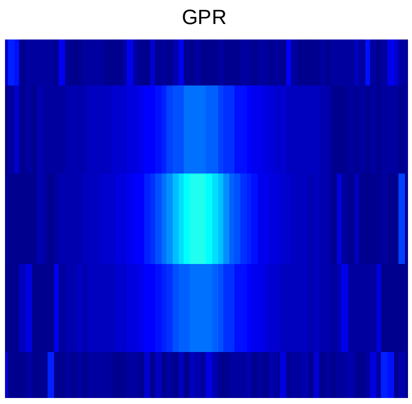

Myopic Action Map

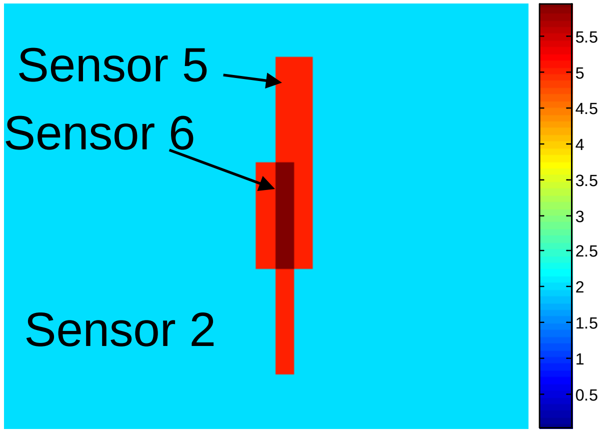

- Shown are the raw signatures from the two sensors and the actions chosen.
- Until the sensors reach the object, Sensor 2 is always chosen. When the object is encountered, Sensor 5 and 6 are deployed.

Confirmation Sensor Scheduling

Iron Clutter Object Example

- Active Sensing estimates the amount of “information gain” achievable from each of the 6 confirmation sensors. Information gain is a measure of the decreased entropy of the state PDF after making an observation.
- Clutter objects (iron, aluminum, and non-metal) have been introduced to study false alarm rejection capabilities of algorithms.

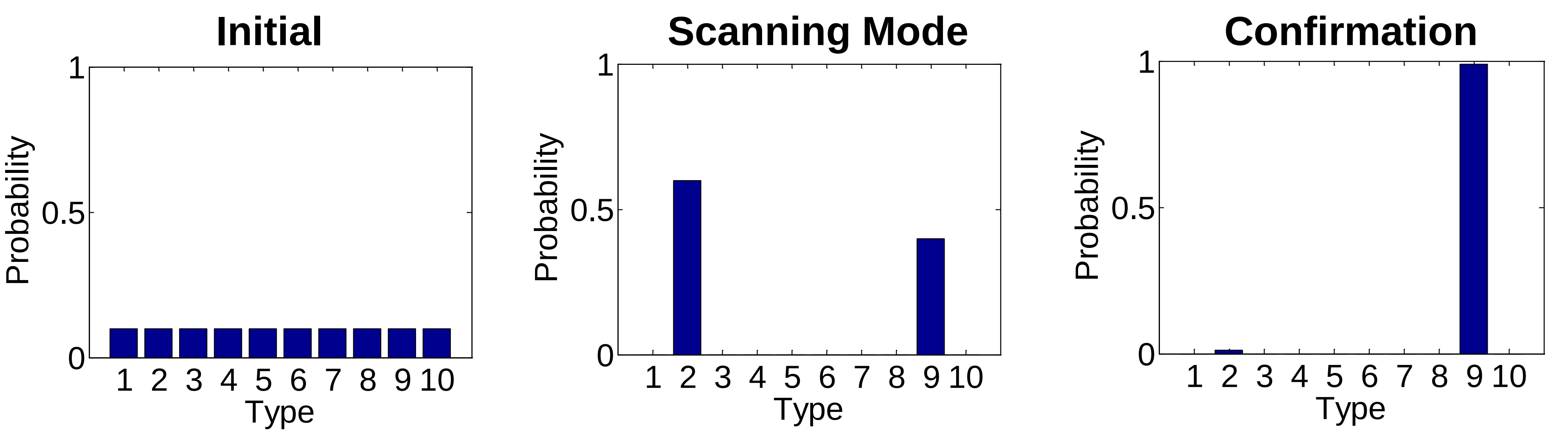

Confusion Matrix after Confirmation

Object Types

X ={1,10}

1 - background

2,3,4 - Metal AT Landmine
deep, mid-depth, shallow

5,6,7 – Low Metal AT Landmine
deep, mid-depth, shallow

Each Row Should Sum to One

	2	3	4	5	6	7	8	9	10
2	1	0	0	0	0	0	0	0	0
3	0	1	0	0	0	0	0	0	0
4	0	0	1	0	0	0	0	0	0
5	0	0	0	0.7	0.3	0	0	0	0
6	0	0	0	0.2	0.8	0	0	0	0
7	0	0	0	0	0.2	0.8	0	0	0
8	0	0.1	0	0	0	0	0.9	0	0
9	0.1	0	0	0	0	0	0	0.9	0
10	0	0	0	0	0	0.2	0	0	0.8

Multiple Confirmation Sensor Scheduling

Downloadable Demo

- Sensors under development at Georgia Tech (Waymond Scott)
- Data set used is the GATech “Three Sensor Dataset” (Feb.2004)
  - Includes metal detector, radar, and seismic vibrometer.
  - Collection performed on three scenarios of mine/clutter arrangements.
  - Data used to guide sensor statistical simulations at U.Mich.

Georgia TECH

Sensors from the Three Sensor Dataset

EMI

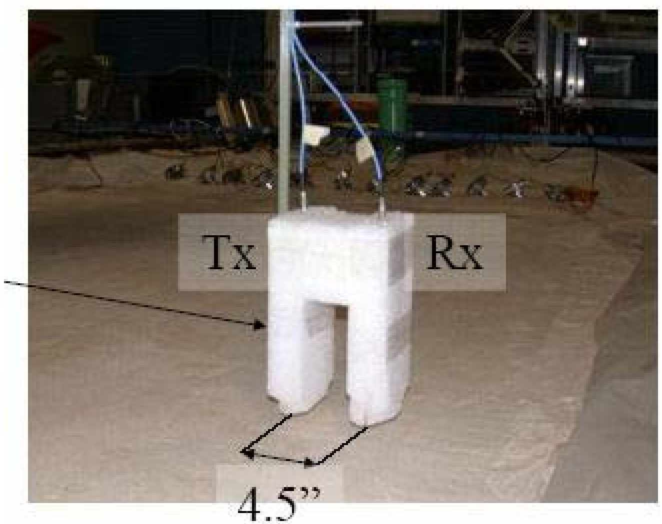

GPR

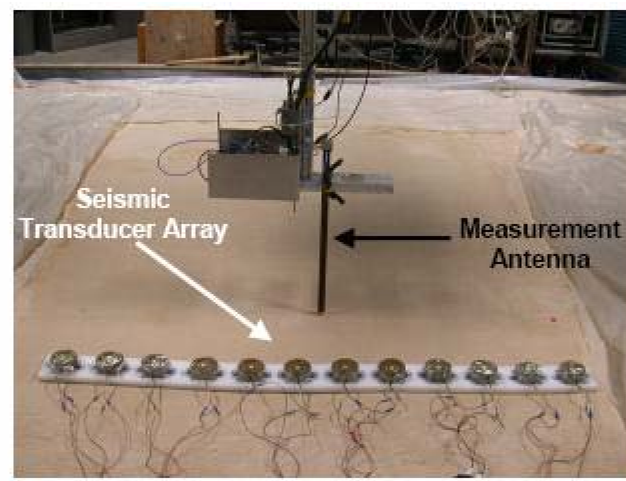

Seismic

Optimal Policy

Assumptions: AT Mines Buried Deep, AP Mines Buried Very Shallow, et.al.

		Object Type								
Sensor		1	2	3	4	5	6	7	8	Feature
		M-AT	M-AP	P-AT	P-AP	Cltr-1	Cltr-2	Cltr-3	Bkg	Description
	EMI	High	High	Low	High	High	Low	Low	Low	Conductivity
		High	High	Low	Medium	Medium	Low	Low	Low	Size
	GPR	High	Low	High	Low	Low	Low	Low	Low	Depth
		High	Medium	High	Medium	Medium	Medium	Medium	Low	RCS
	Seismic	Medium	High	Medium	High	Medium	Medium	Low	Low	Resonance
		1 D	1 D	1 2 D	1 2 3 D	1 2 3 D	1 D	1 D	1 D	

1 – EMI
2 – GPR
3 – Seismic
D – Make Decision

Cltr1 – Hollow Metal
Cltr2 – Hollow Non-metal
Cltr3 – Non-hollow Non-metal

Performance Comparison (Pc vs E[N])

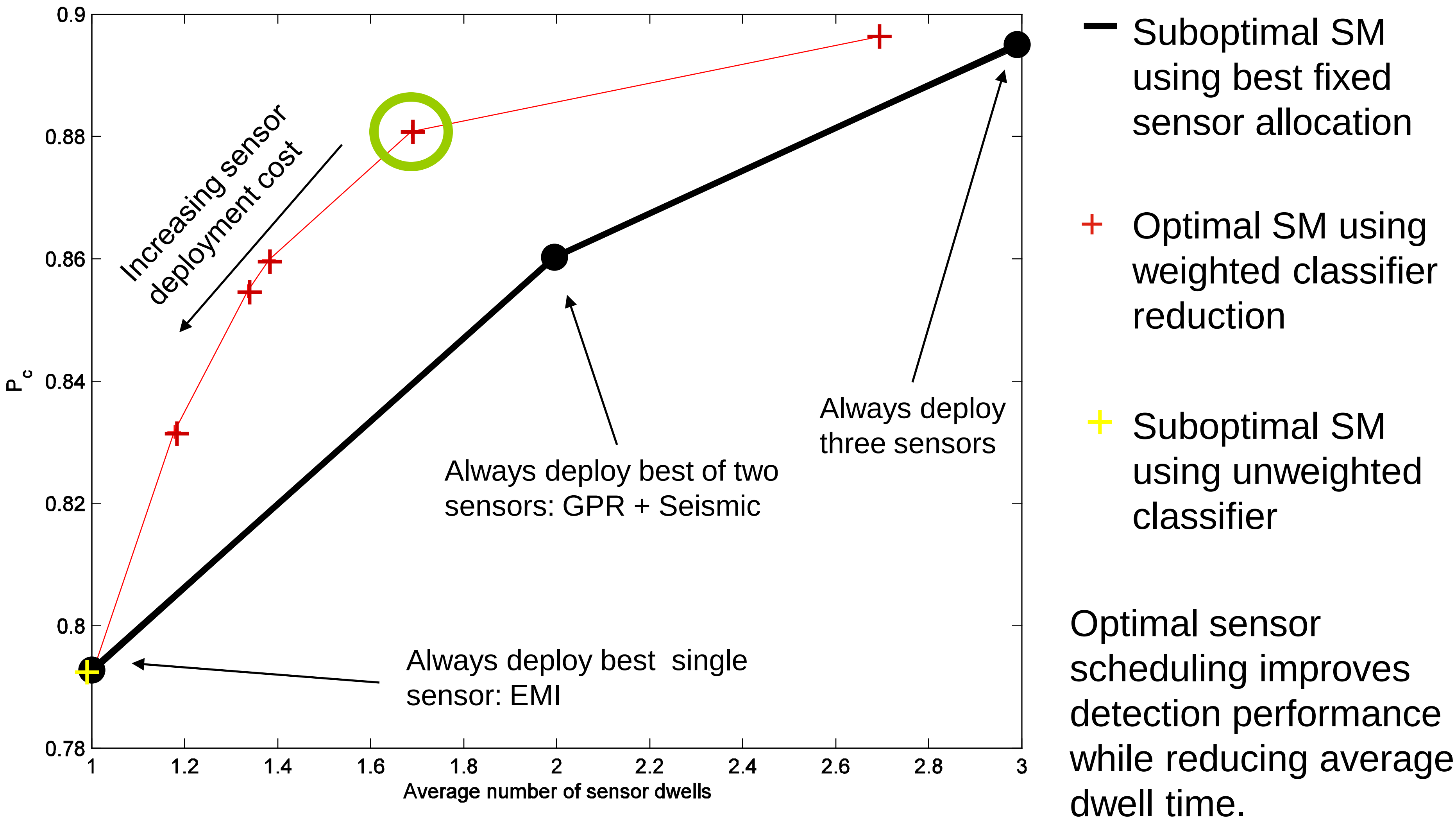

Optimal sensor scheduling improves detection performance while reducing average dwell time.

Statistical Contributions

- Marble,J., Blatt,D., Hero,A., ``Confirmation Sensor Scheduling using a Reinforcement Learning Approach,'' SPIE: Detection and Remediation Technologies for Mines and Minelike Targets XI, March 2006, Orlando, FL.

- Marble,J., Yagle,A., Hero,A, ``Sensor Management for Landmine Detection,'' SPIE: Detection and Remediation Technologies for Mines and Minelike Targets X, March 2005, Orlando, FL.

- Marble,J., Yagle,A., Hero,A, ``Multimodal, Adaptive Landmine Detection Using EMI and GPR,'' SPIE: Detection and Remediation Technologies for Mines and Minelike Targets X, March 2005, Orlando, FL.

Imaging

See-Through-Wall Radar
and Volumetric Landmine Imaging

Imaging

- I.R.I.S. Adaptive Imaging
  - Iterative Redeployment of Imaging and Sensing
  - Adaptively build a large scene out of small aperture radar measurements.
  - Use sensor scheduling to redeploy small aperture radar.
- Phase Delay Estimation and Correction
  - Two methods proposed for homogeneous external walls.
  - The magic parameter: $\tau\sqrt{\varepsilon_2}$
  - Autofocus techniques required in real world system.
- Near Real Time Imaging of Large Scenes
  - 2D for STW and 3D for Landmine
  - Matrix Implementation of Wavenumber Migration
  - Development of a Forward Operator by “Reverse Engineering” the Adjoint Operator

See-Through-Wall Radar Imaging

SRI International Building 409
Menlo Park, CA

- SRI Sidelooking Radar
- Monostatic SAR
  - Fully Polarimetric: HH, VV, HV
- Frequencies
  - 800-2400 MHz
  - 301 Frequency Steps
- Antenna Height 7.5m

See-Through-Wall Radar Imaging

Wavenumber Migration Image

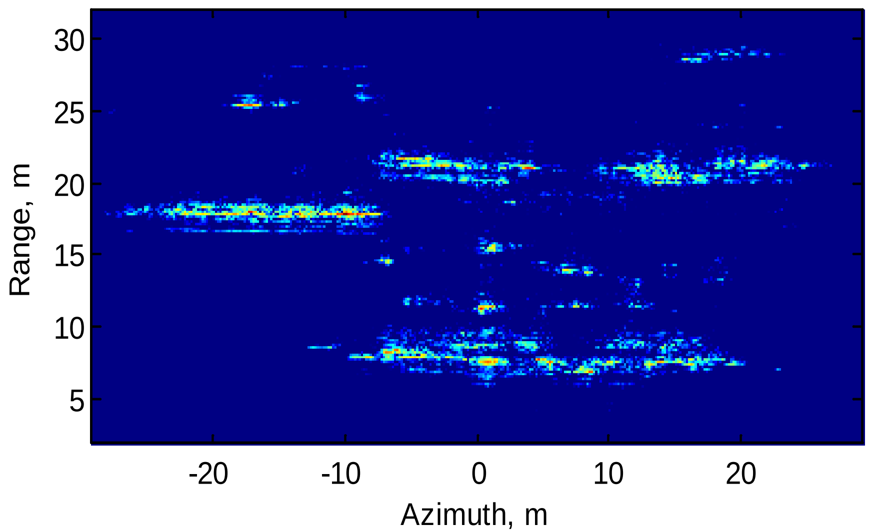

Raw Data

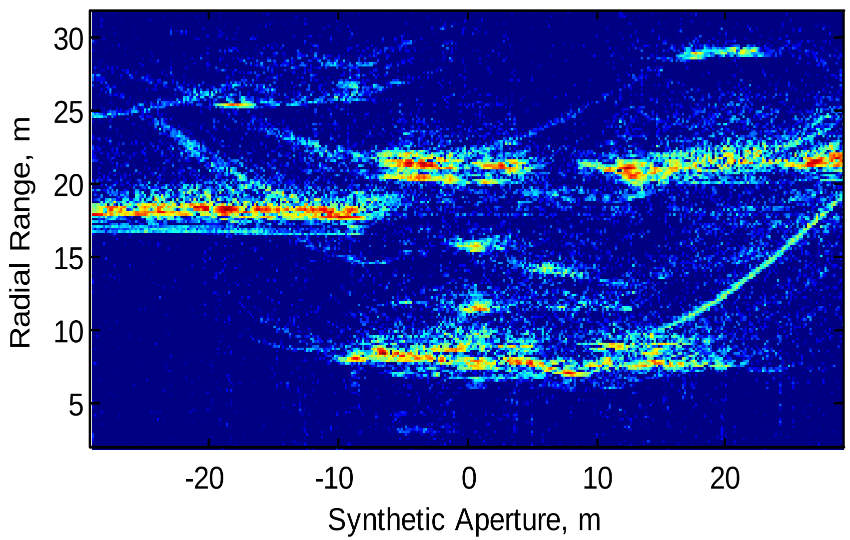

SRI International Building 409
Menlo Park, CA

- SRI Sidelooking Radar
- Monostatic SAR
  - Fully Polarimetric: HH, VV, HV
- Frequencies
  - 800-2400 MHz
  - 301 Frequency Steps
- Antenna Height 7.5m




See-Through-Wall Radar Imaging

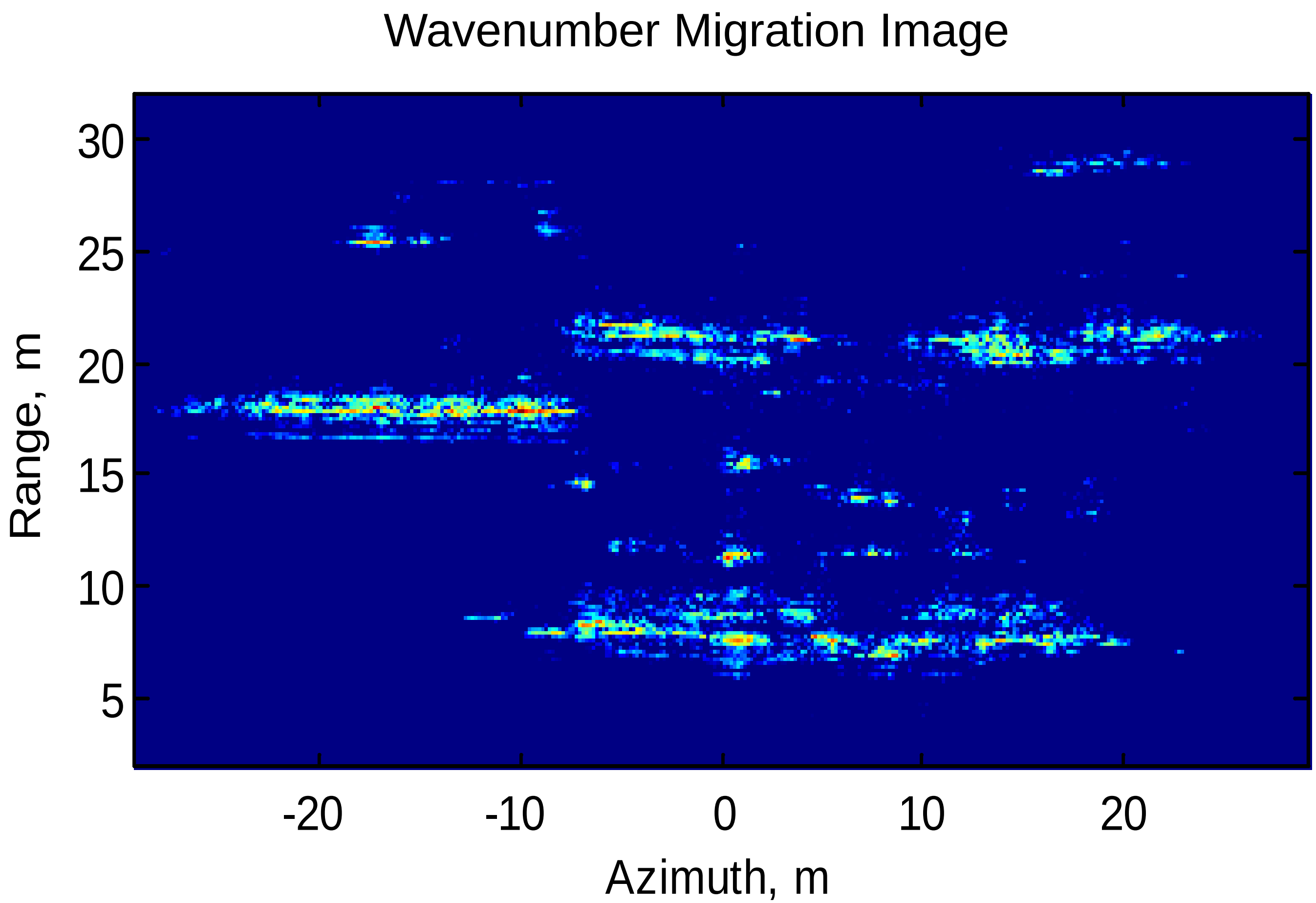

See-Through-Wall Radar Imaging

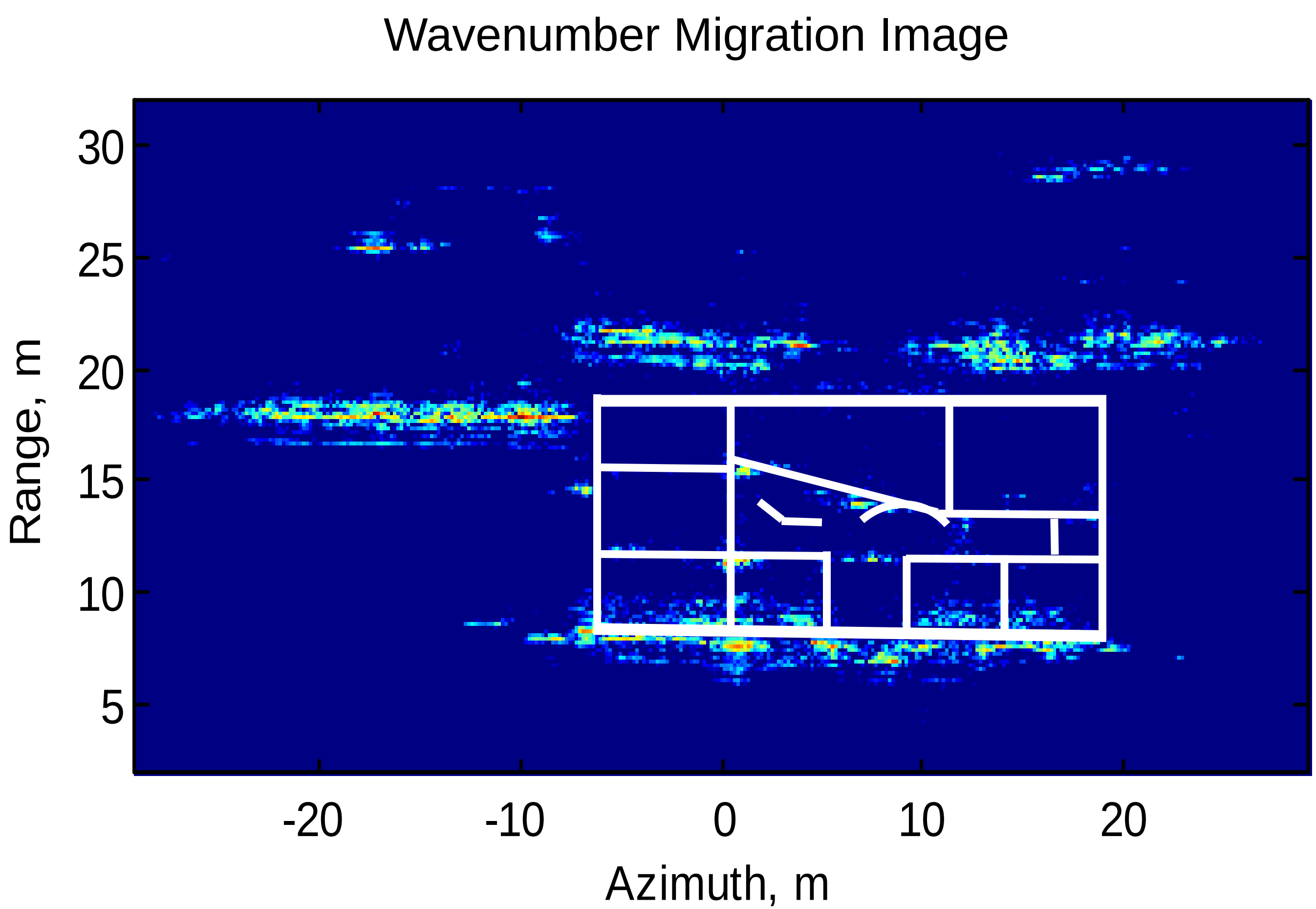

Floor Plan

Iterative Redeployment of Illumination and Sensing

Elements of the I.R.I.S. Strategy

- **Initial illumination with physical antenna array**
  - Antenna array is deployed at an initial location and illuminates the region of interest.
  - Sparse reconstruction image reconstruction (Ting:2006) is performed
- **Form Confidence Map of Image**
  - Confidence map (Raich:2005) is computed using initial image and side information
  - Select a region of low confidence from confidence map
- **Simulate external energy/resolution field induced by virtual transmitter**
  - Place virtual transmitter in low confidence region and apply FEM, MoM, PO to estimate electric field distribution outside the building
  - Compute induced energy or gradient field (wrt perturbation of virtual transmitter location)
- **Re-illuminate with physical antenna array at maximum of simulated field**

Sensor Illumination

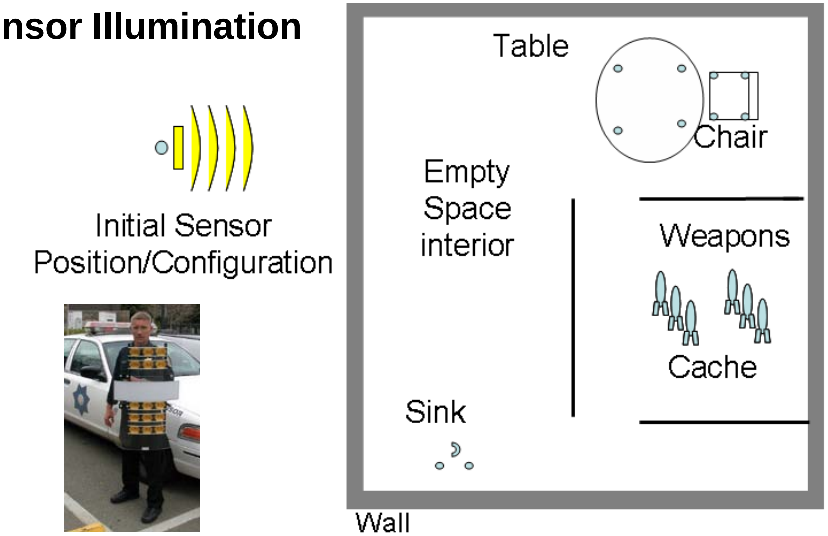

Uncertainty Map

Predict Information Gain

(Energy or Resolution MAP)

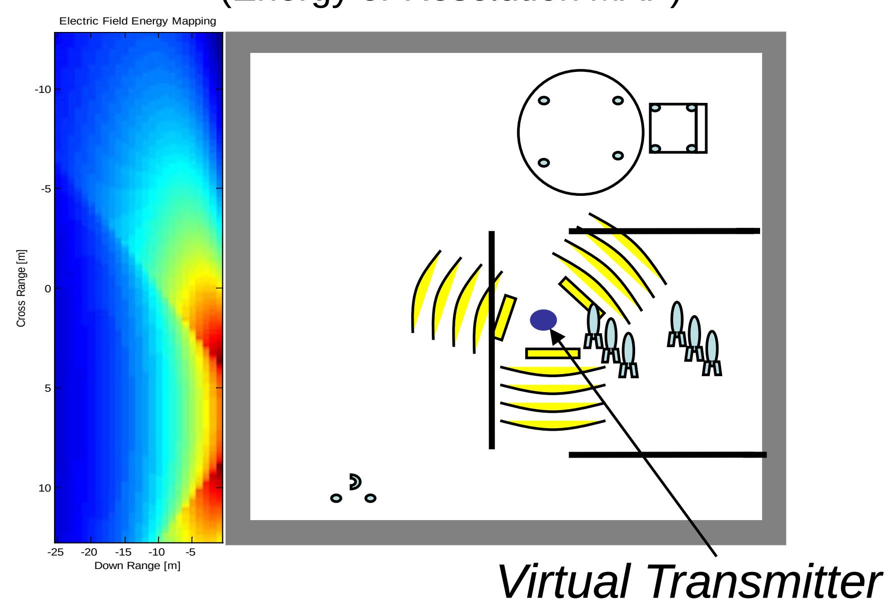

IRIS Simulation

Standard Scene

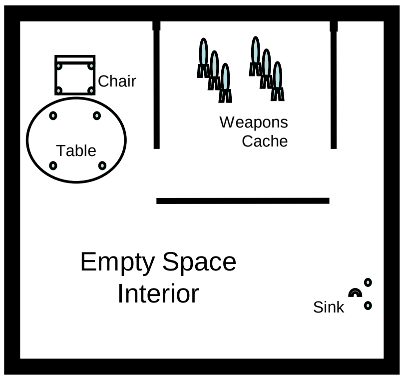

- IRIS Simulation for Proof of Concept
- Bandwidth: 4-5GHz
- Number Frequencies: 512
- Aperture per side: 10m
- Full Synthetic Array: 512 elements
- Subaperture Array: 50 elements

Full ISAR Image

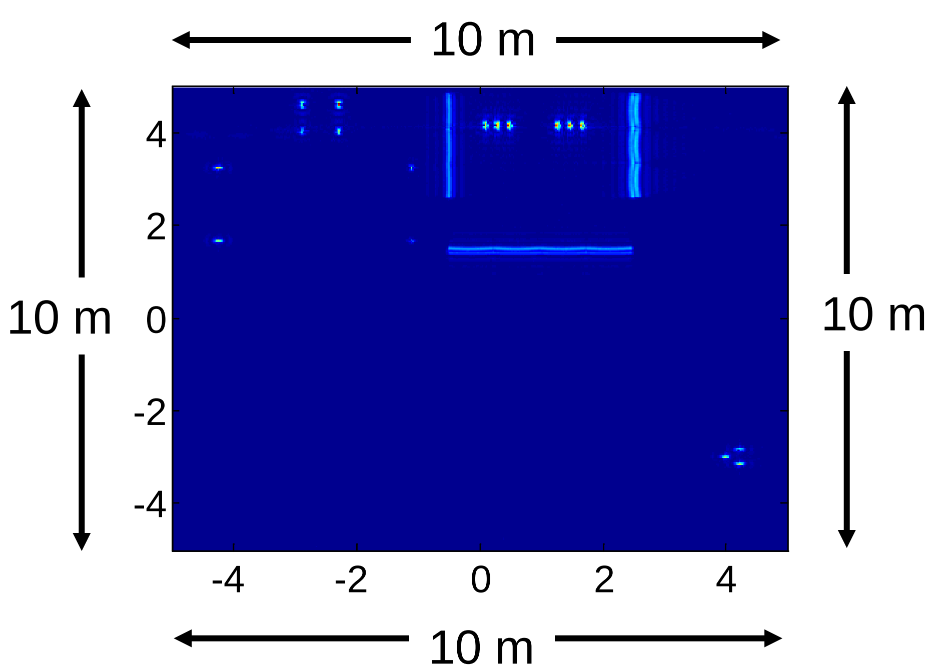

Total Aperture: 40m

Adaptive IRIS Image

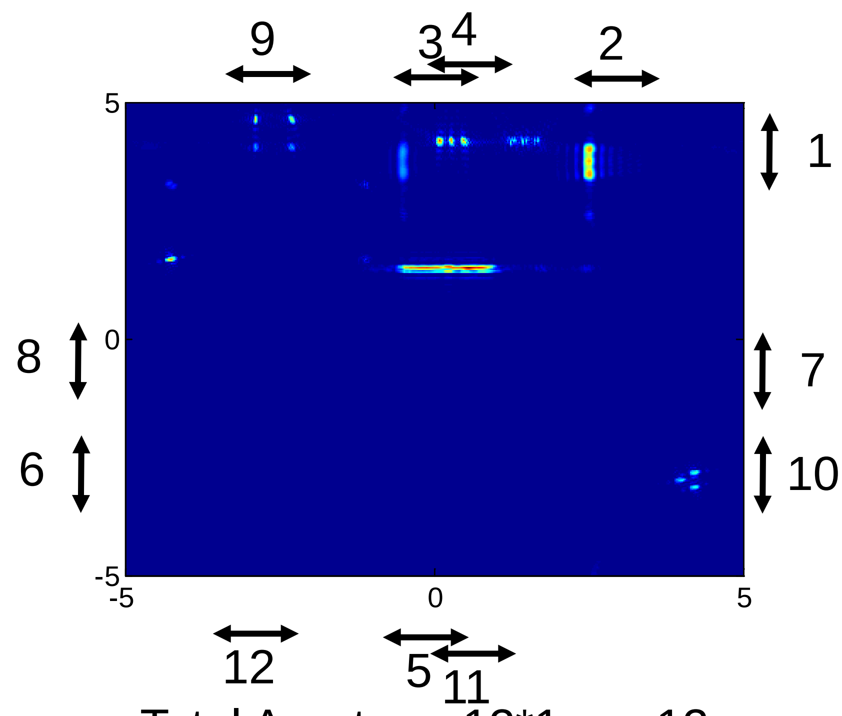

Total Aperture: 12*1m = 12m

IRIS "Modules"

- Uncertainty Map – Inside Building
  - The Ting Method
  - The Yuan&Lin (inspired) Method

  Both Used in automated IRIS
- Sensor Information Map – Outside Building
  - KL Divergence Metric (Max Info Gain)
  - Energy Method (Max SNR)

  Both Used
- Virtual Transmitter
  - Currently using "Enhanced Geometrical Optics"
    - A high frequency approximation.
    - Mathematically simple and fast
    - Valid (and possibly only choice) at higher frequencies
    - Not valid at corners
  - Other Methods – Numerically Intense
    - All require 10 samples per (shortest) wavelength
    - MoM, FEM, FDTD
- The Observations
  - Simulated – Currently using Enhanced Geometrical Optics
  - Real Data – Always best.
- Imaging
  - Sparse Reconstruction Based on Wavenumber Migration
  - Other's can be substituted based on performance characteristics.

Uncertainty Map

Confidence

$$P(I=0|z) = \frac{\frac{1-w}{\sqrt{2\pi\sigma^2}} e^{-\frac{z^2}{2\sigma^2}}}{f_Z(z)} \quad \text{(Ting\&Hero)}$$

$$f_Z(z) = \frac{1-w}{\sqrt{2\pi\sigma^2}} e^{-\frac{z^2}{2\sigma^2}} + \frac{aw}{4}\left(\left(\left(1-\operatorname{erf}\left(\frac{a\sigma+\frac{z}{\sigma}}{\sqrt{2}}\right)\right)e^{\frac{a^2\sigma^2+2az}{2}} + \left(1+\operatorname{erf}\left(\frac{\frac{z}{\sigma}-a\sigma}{\sqrt{2}}\right)\right)e^{\frac{a^2\sigma^2-2az}{2}}\right)\right)$$

$$erf(x) = \frac{2}{\sqrt{\pi}} \int_{t=0}^{x} e^{-t^2} dt$$

Entropy

$$p = P(I=0\,|\,z)$$

$$S(p) = -p\log_2(p) - (1-p)\log_2(p)$$ ← Final uncertainty mapping (Map #1)

Ting,M, Hero,A.O., “Sparse Image Reconstruction Using a Sparse Prior,” IEEE International Conference on Image Processing, Atlanta, GA, Oct. 8-11, 2006.

Uncertainty Map

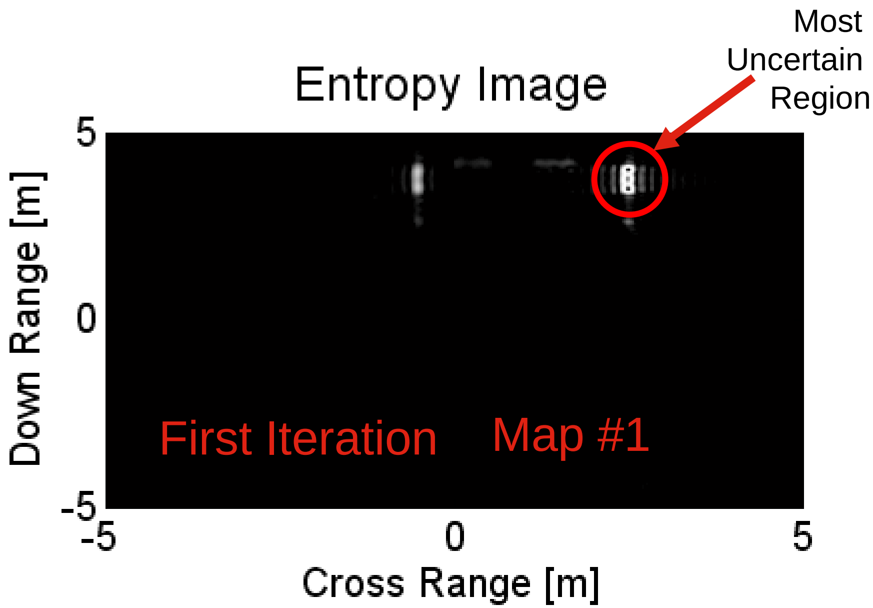

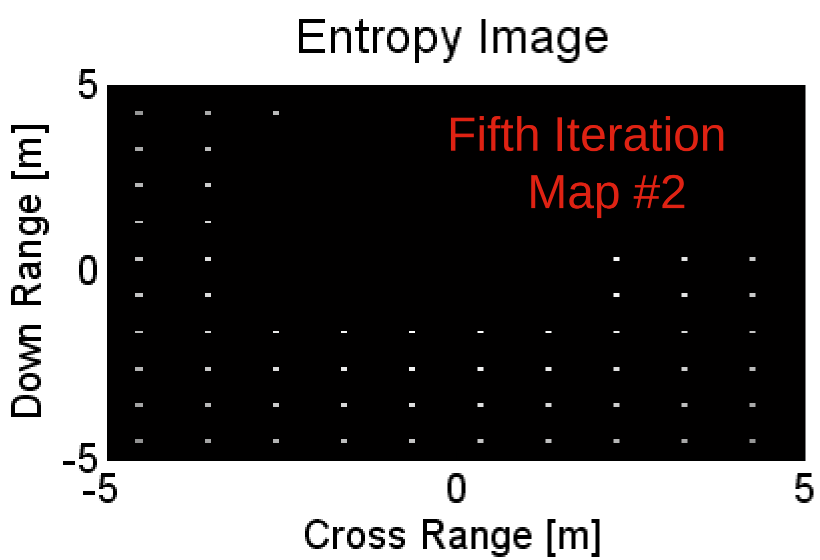

- Uncertainty Map shows pixels that are likely to be "empty".
- Regions of the image that have not been viewed by the sensor are accounted for by the second Uncertainty Map. This second map is inspired by Yuan&Lin (JASA 2005).
- Note: Pixels are *Directional* Meaning that radar images are composed of directional scatterers.

Sensor Information Map

Kullback Leibler Divergence – Information Gain

Observation Location

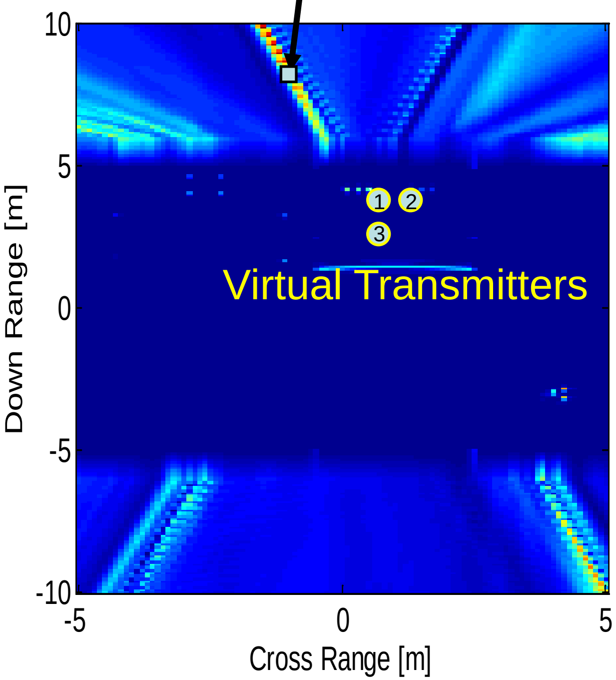

$\vec{E}_k$ -Electric Field From Transmitter k.

$$\mathrm{Div}(E_k, E_j) = \left|\vec{E}_j\right| \log\left(\frac{\left|\vec{E}_j\right|}{\left|\vec{E}_k\right|}\right)$$

$$\text{Div Map} = \mathrm{Div}(E_1,E_3) + \mathrm{Div}(E_1,E_2)$$

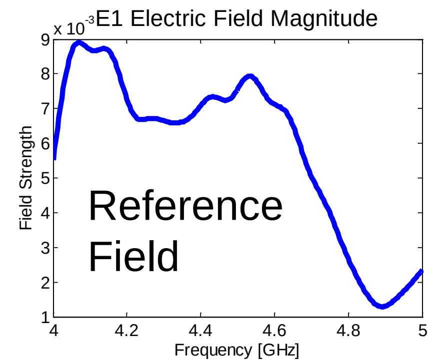

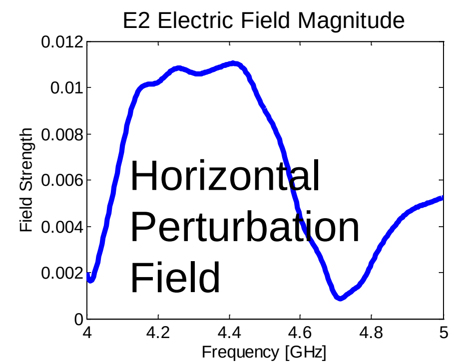

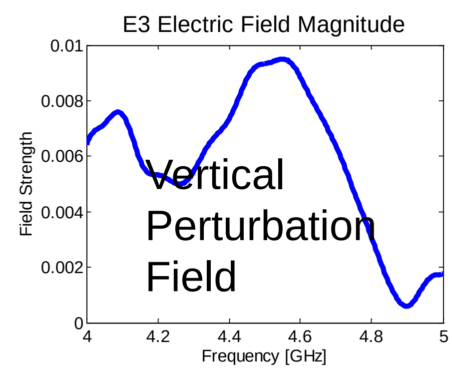

"Enhanced" Geometrical Optics

Observations

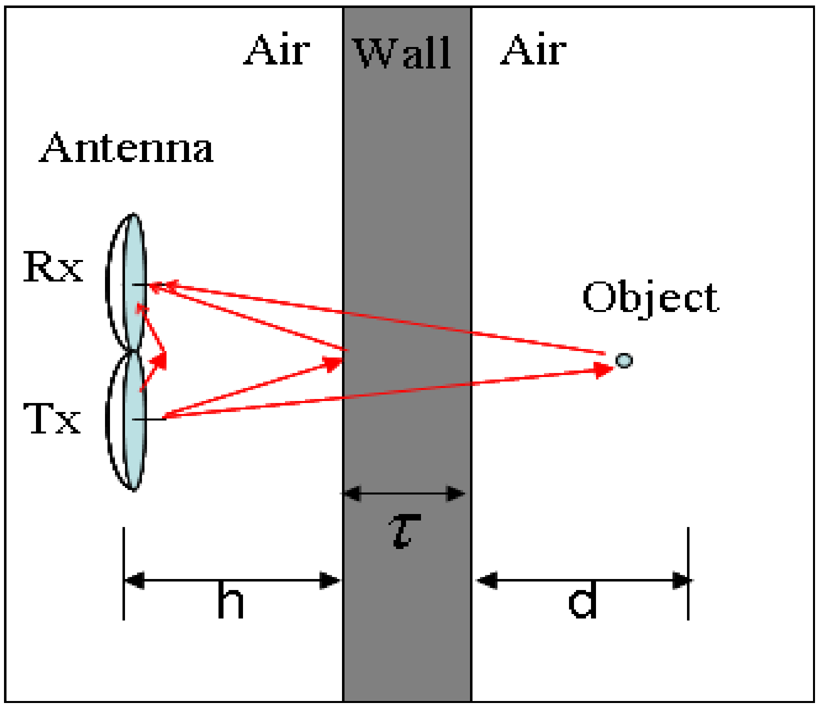

Virtual Transmitter

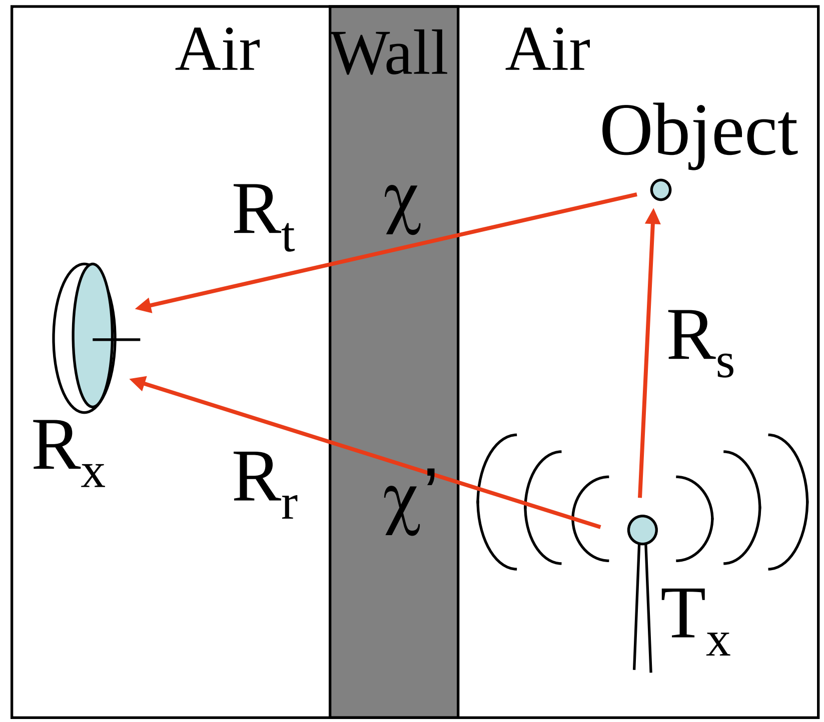

Virtual Transmitter

“Enhanced” Geometrical Optics

(Direct Path from Transmitter)

$$E'_R(f,x) = E_0\left(\sqrt{\frac{G_T G_R \lambda^2}{(4\pi R_r)^2}}\right) T'_{12}\, T'_{21}\, e^{-\alpha\chi} e^{-j\beta\chi} e^{-jk(R_r-\chi)}$$

(response from object)

$$E_R(f,x) = E_0\left[\left(\sqrt{\frac{G_T G_R \lambda^2}{\left((4\pi)^3 R_s^2 R_t^2\right)}\sigma_{RCS}}\right) T_{12} T_{21} e^{-\alpha\chi} e^{-j\beta\chi}\right] e^{-jk(R_s+R_t-\chi)}$$

G_T – Gain of transmit antenna
G_R – Gain of receive antenna
E_R – Electric field strength at the receiver
E_0 – Transmitted Electric field strength.
h – Height of antenna above ground
d – Depth of target below the surface
λ – Wavelength in Free Space
σ_{RCS} – Target Radar Cross Section

$$k = \sqrt{\omega^2 \mu_0 \varepsilon_0}$$ (Propagation Constant in Free Space)

χ – Distance Inside Wall

f – Frequency of Plane Wave

x – Location in Aperture

Observations

“Enhanced” Geometrical Optics

(response from wall interface)

$$E'_R(f,x) = E_0\left[\left(\sqrt{\frac{G_T G_R}{\left(4\pi h^2\right)^2}\left(\frac{\lambda^2}{4\pi}\right)}\right)R_{12}\right]e^{-j2kh}$$

(response from object)

$$E_R(f,x) = E_0\left[\left(\sqrt{\frac{G_T G_R}{\left(4\pi R^2\right)^2}\left(\frac{\lambda^2}{4\pi}\right)\sigma_{RCS}}\right)T_{12}^2 T_{21}^2 e^{-2\alpha\chi}e^{-j2\beta\chi}\right]e^{-j2k(R-\chi)}$$

G_T – Gain of transmit antenna
G_R – Gain of receive antenna
E_R – Electric field strength at the receiver
E_0 – Transmitted Electric field strength.
h – Height of antenna above ground
R – Total distance to target
λ – Wavelength in Free Space
σ_{RCS} – Target Radar Cross Section

$$k = \sqrt{\omega^2 \mu_0 \varepsilon_0}$$ (Propagation Constant in Free Space)

χ – Distance Inside Wall

f – Frequency of Plane Wave

x – Location in Aperture

“Enhanced” Geometrical Optics

Fresnel Reflection and Transmission Coefficients

$$R_{12} = \frac{1 - \frac{1}{\sqrt{\varepsilon_r}}}{1 + \frac{1}{\sqrt{\varepsilon_r}}}$$

$$T_{12} = \frac{2}{1 + \frac{1}{\sqrt{\varepsilon_r}}}$$

$$T_{21} = \frac{2}{1 + \sqrt{\varepsilon_r}}$$

Attenuation and Propagation Constants in Conducting Media

$$\alpha = \omega\sqrt{\mu\varepsilon}\left[\frac{1}{2}\left(\sqrt{1 + \frac{\sigma^2}{\varepsilon^2\omega^2}} - 1\right)\right]^{\frac{1}{2}}$$

$$\beta = \omega\sqrt{\mu\varepsilon}\left[\frac{1}{2}\left(\sqrt{1 + \frac{\sigma^2}{\varepsilon^2\omega^2}} + 1\right)\right]^{\frac{1}{2}}$$

$$\beta \approx \omega\sqrt{\mu\varepsilon}\sqrt{\varepsilon_r}$$

Slightly Conducting Media Approximation

IRIS DEMO

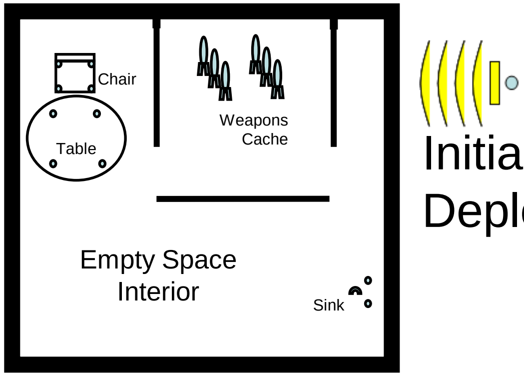

Initial
Deployment

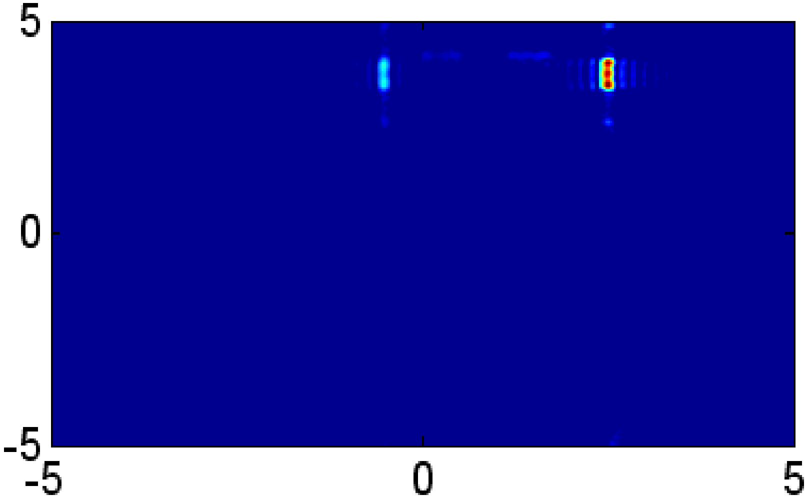

Iteration #1

IRIS DEMO

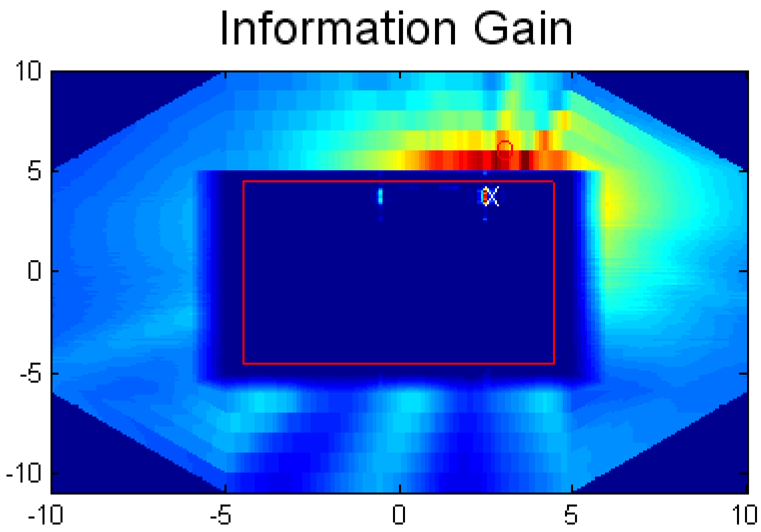

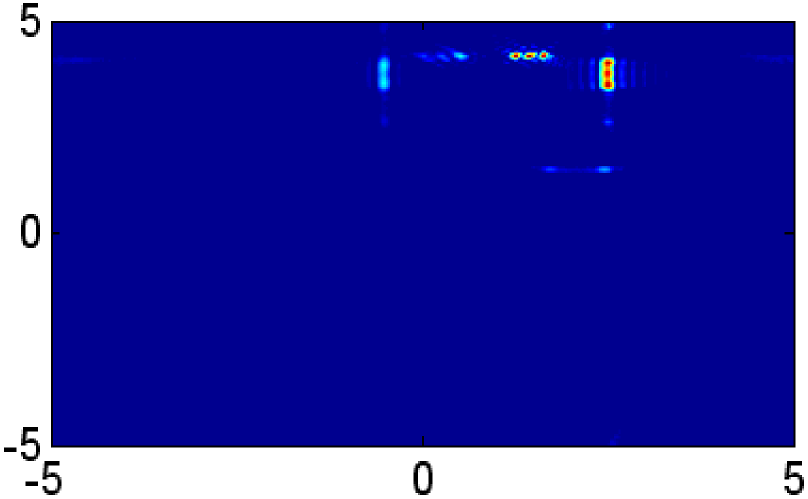

Iteration #2

IRIS DEMO

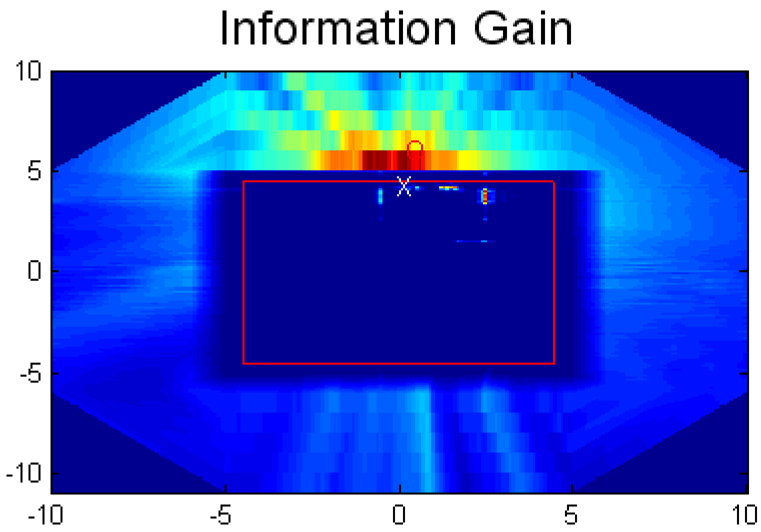

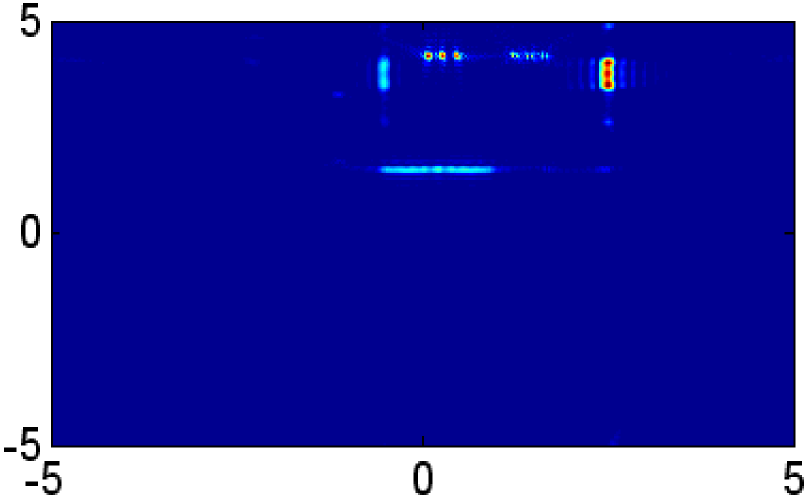

Iteration #3

IRIS DEMO

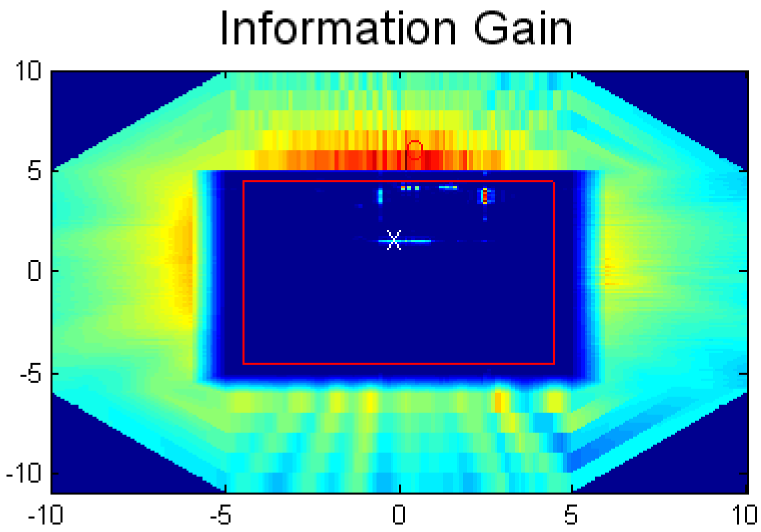

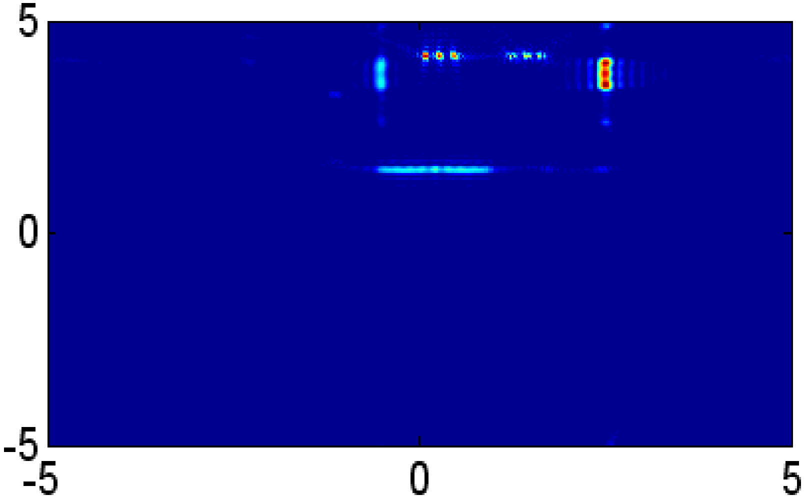

Iteration #4

IRIS DEMO

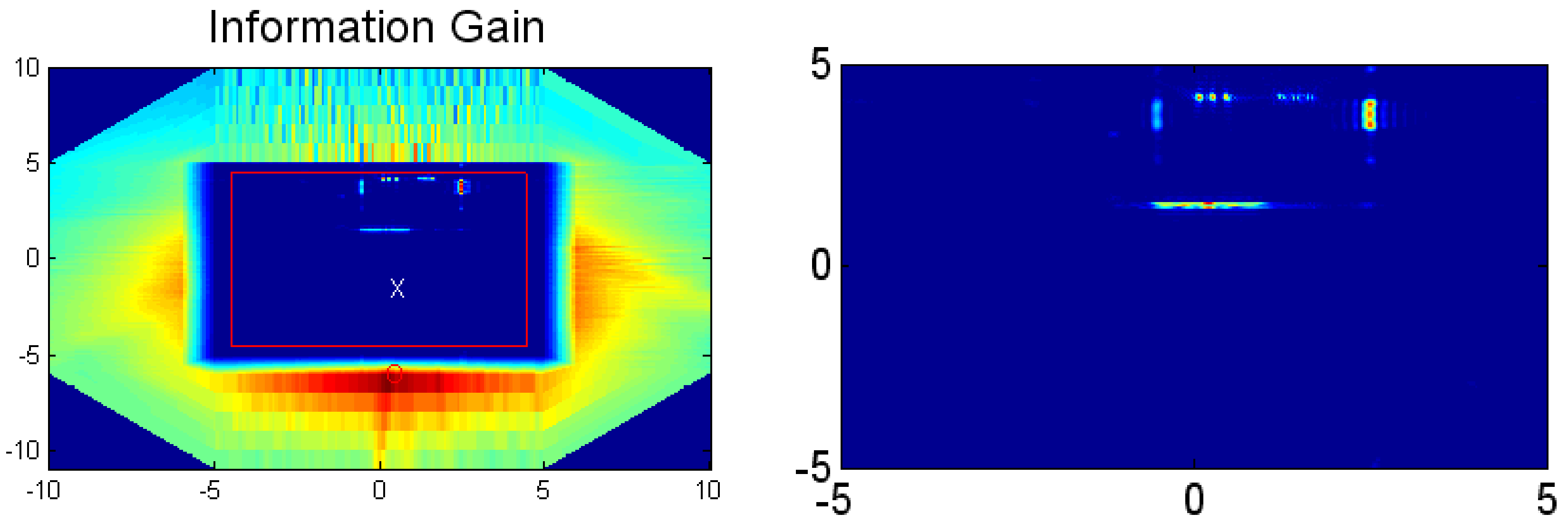

Iteration #5

IRIS DEMO

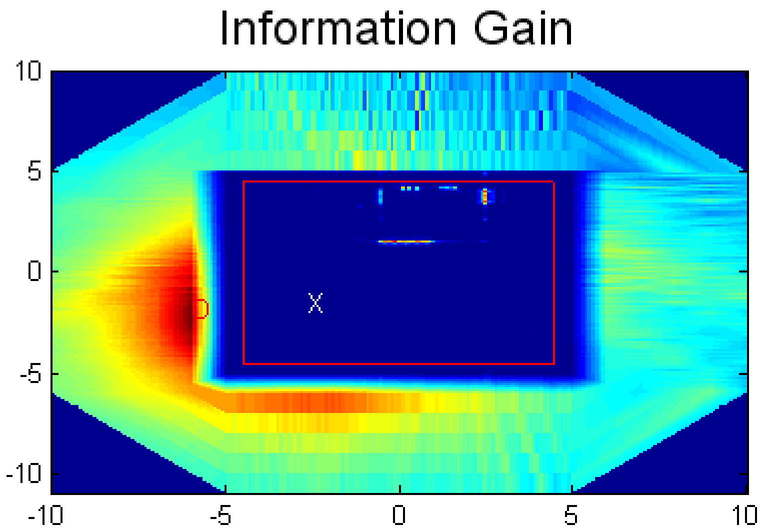

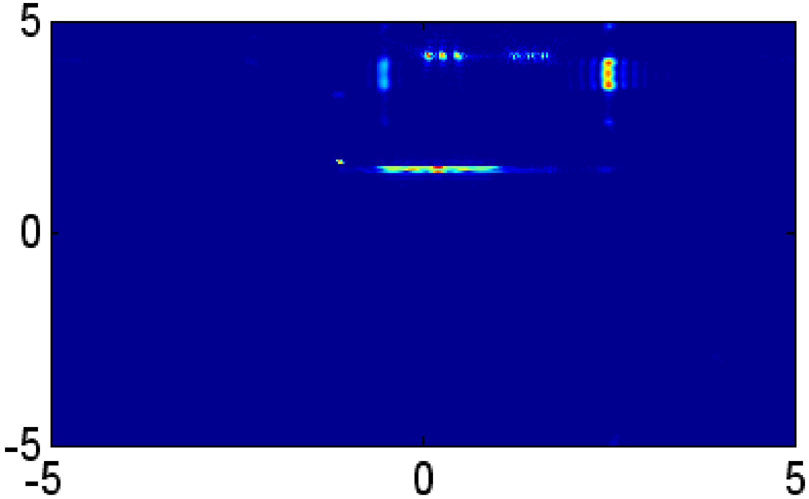

Iteration #6

IRIS DEMO

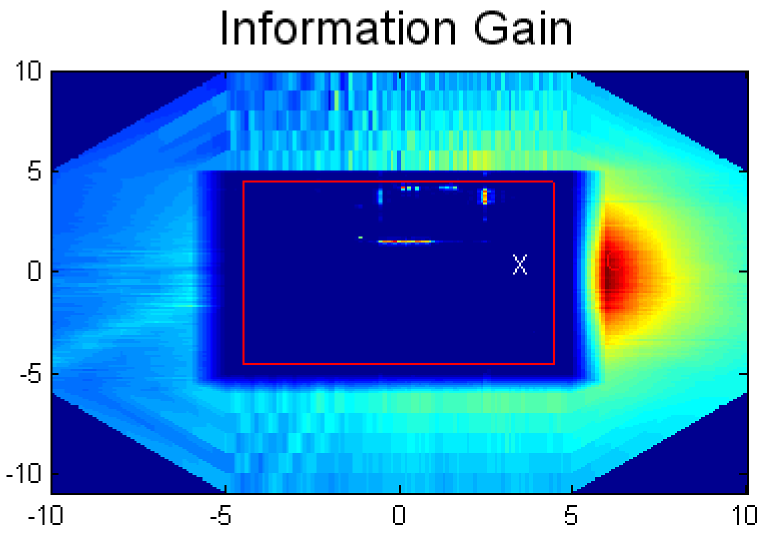

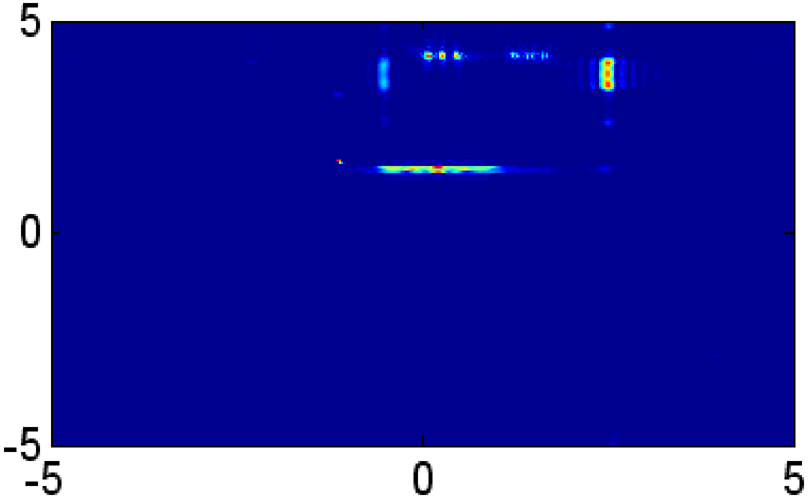

Iteration #7

IRIS DEMO

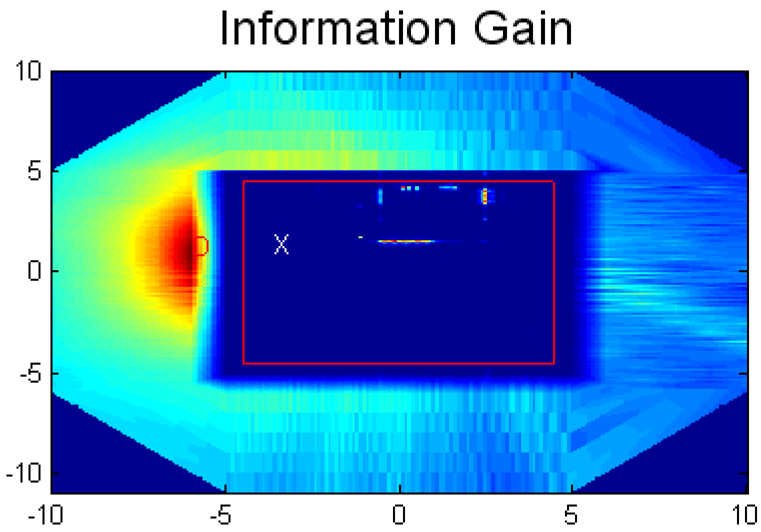

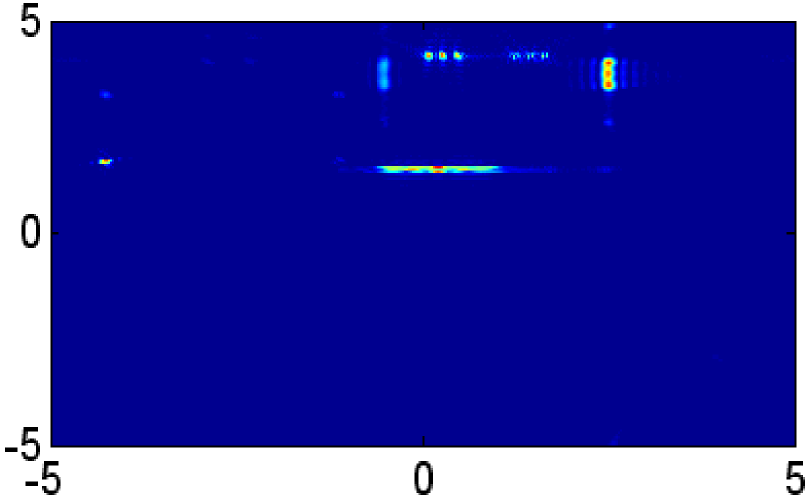

Iteration #8

IRIS DEMO

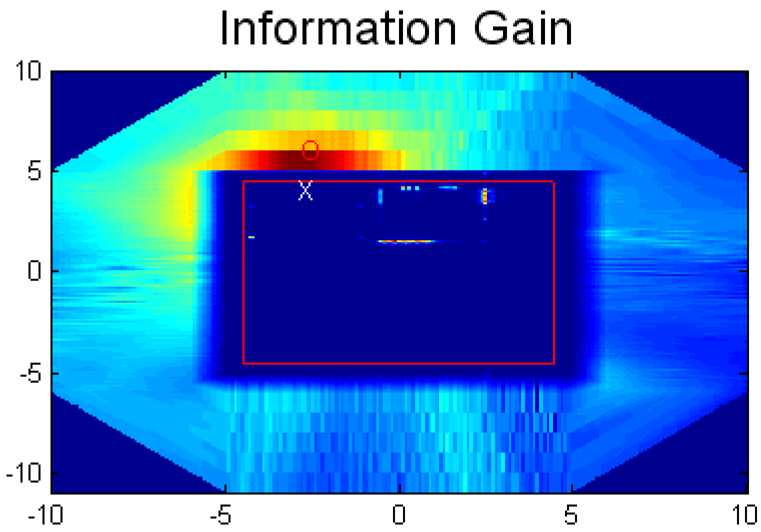

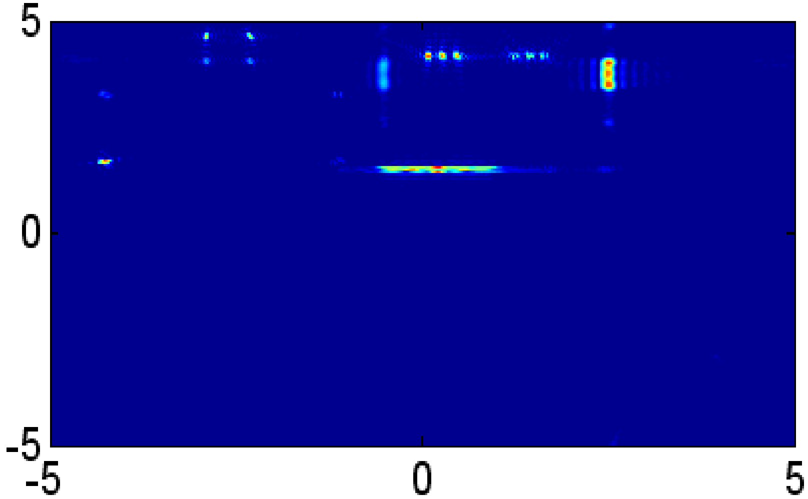

Iteration #9

IRIS DEMO

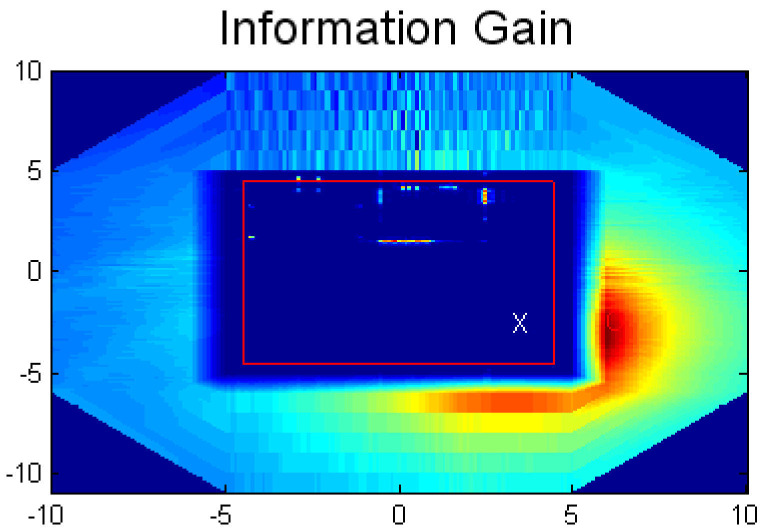

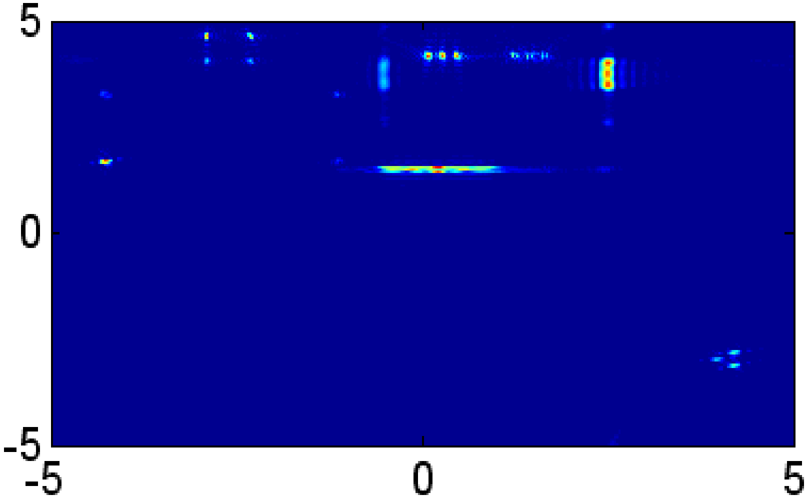

Iteration #10

IRIS DEMO

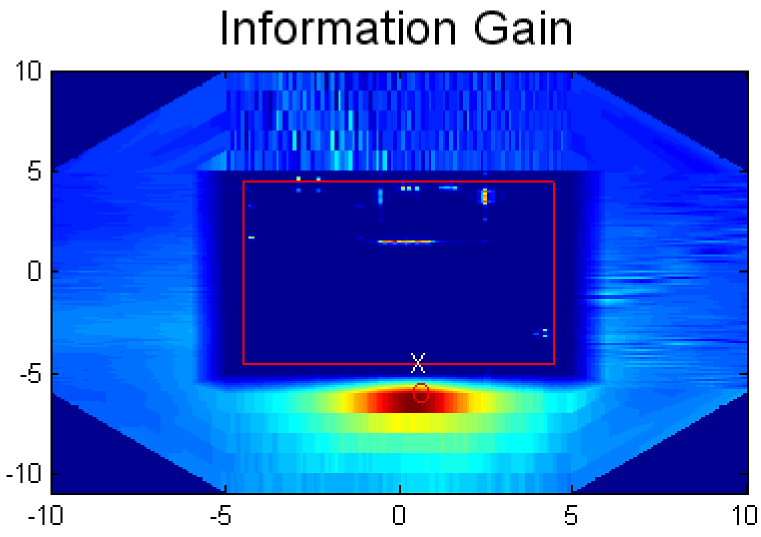

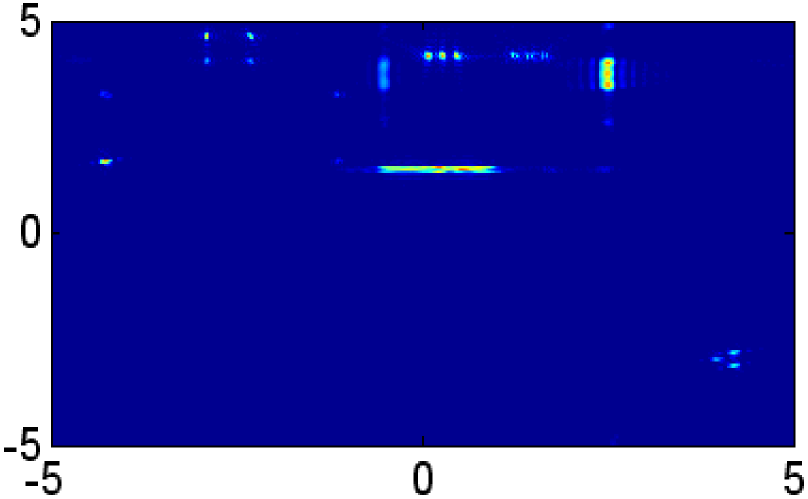

Iteration #11

IRIS DEMO

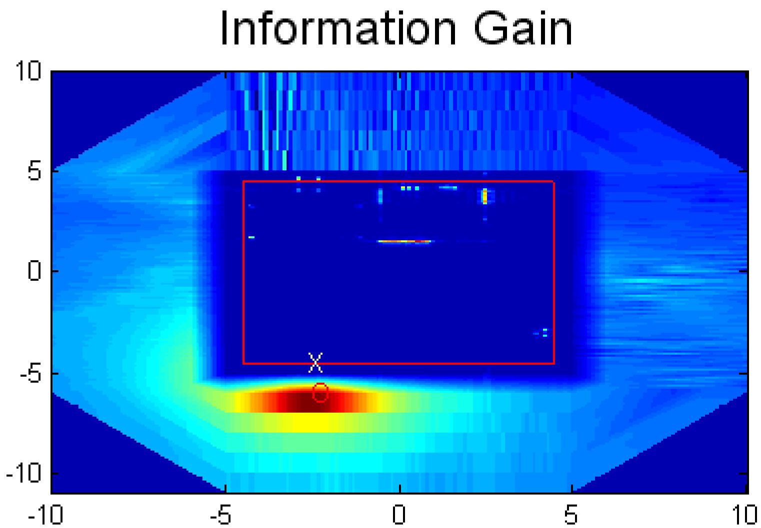

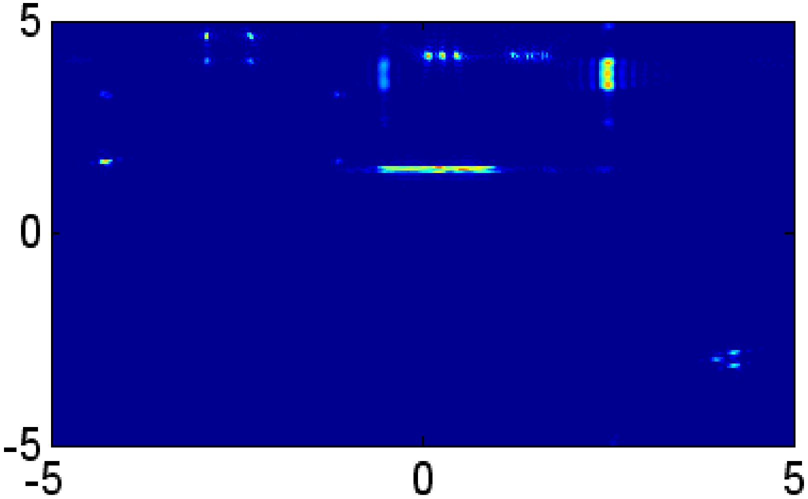

Iteration #12

IRIS DEMO

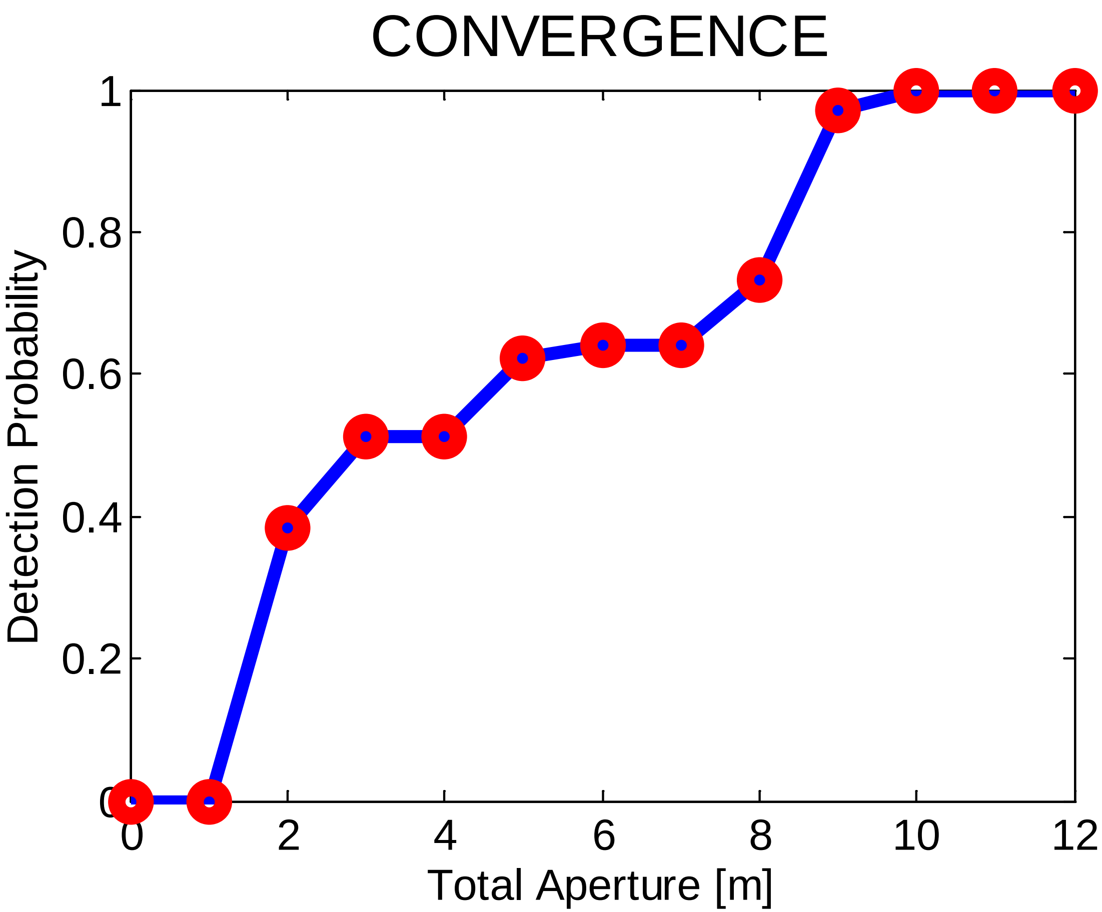
CONVERGENCE
Detection Probability
0
0.2
0.4
0.6
0.8
1
0
2
4
6
8
10
12
Total Aperture [m]

Imaging

Backpropagation SAR Imaging

Scene Grid

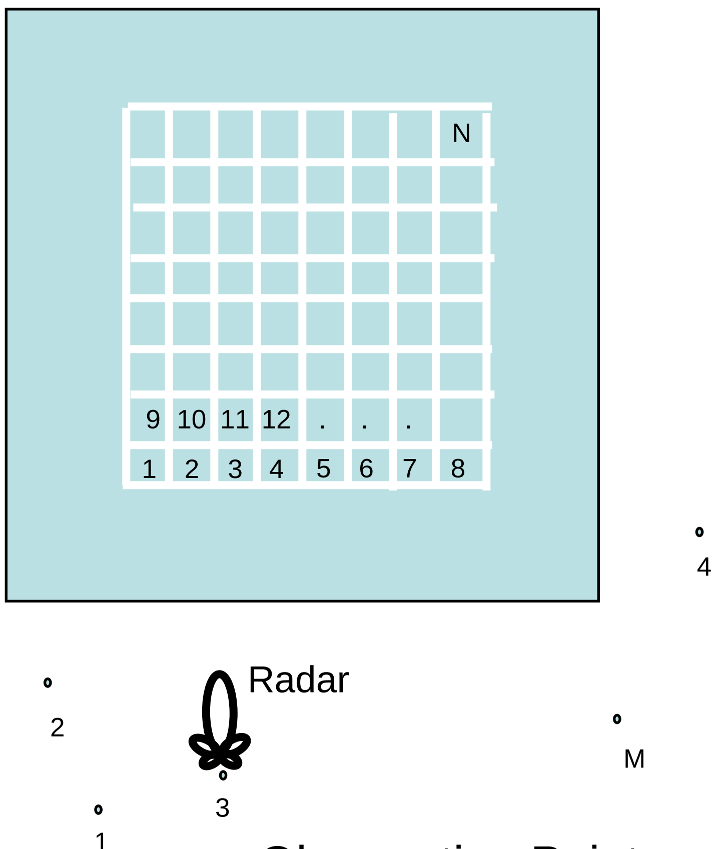

Observation Points
(Non-uniformly Spaced)

$\underline{y}$ - Observation Vector

- Collected by the sensor
- Monostatic or Bistatic
- Multiple locations and frequencies
- Can be uniformly or non-uniformly spaced, but locations must be known.

$\underline{x}$ - Scene Vector

- *Vectorized* version of the scene.
- Goal is to reconstruct this vector from the observations.

$$\hat{x}_n = \sum_{m=1}^{M} R_{mn} e^{+j\frac{4\pi f_0}{c}R_{mn}} y_m$$

R_{mn} is sometimes ignored.

Imaging

- Small Image (100 x 100 pixels) for discussion
- Looping (Desktop PC -2.2GHz, 2.0GBytes, 1-64bit - processor)
  - MATLAB 11 min 16 sec
  - ANSI C: 1 min 1 sec
- MATLAB (Matrix Multiplication – 1 processor)
  - Desktop PC (2.2GHz, 2.0GBytes, 1-64bit - processor) : OUT OF MEMORY
  - Lab PC (3.5GHz, 3.5GBytes, 1 processors): OUT OF MEMORY
  - Lab PC Linux (3.5GHz, 4GBytes, 1 processor): 1.7 sec
  - HPC (Linux Networx Evolocity II – 1 node): 2.7 sec
- MATLAB (Matrix Multiplication Multithreading – 2 processors)
  - MAC (2GHz, 2GBytes, 2 processors) 1.05 sec
  - Linux (3.5GHz, 4GBytes, 2 processors) 0.95 sec
- MATLAB (FFT Acceleration)
  - Wavenumber Migration (Multithreading - 2 processors) 0.09 sec

35x

1.8x

10x

Imaging

Wavenumber Migration

An Efficient Form of Backpropagation

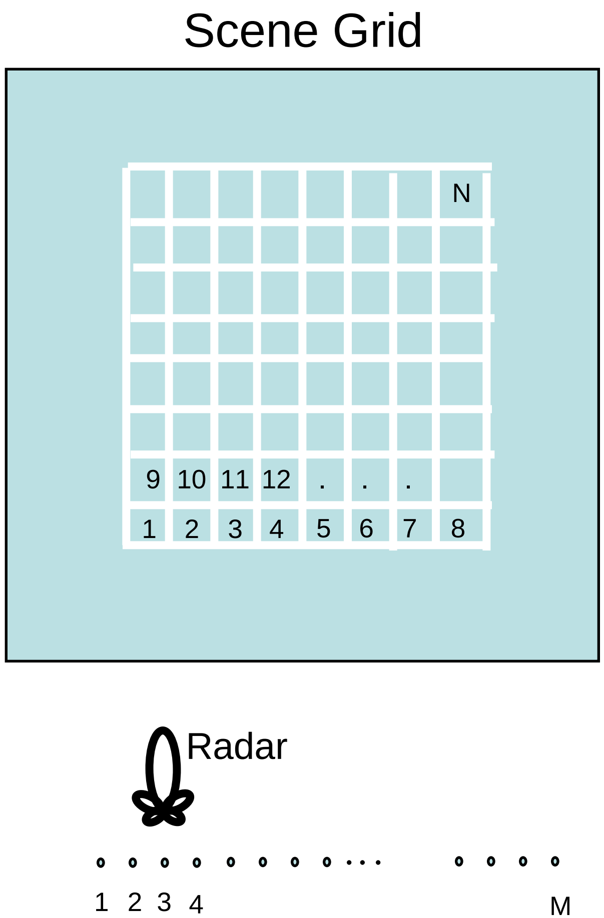

Observation Points in Regular Array

$\underline{y}$ - Observation Vector

- Observation points are now made along a regular spaced array.
- This allows, with some modification to the observations, for the use of an FFT when forming the image.

$$\hat{\underline{x}} = FFT^{-1}\left[f\left(\underline{y}\right)\right]$$

$f(\underline{y})$ – Modification to the observations

- Since the observations are not quite the Fourier transform of the scene, a correction must be made to the data.
- The proper modifications are performed by the function f(.).

Imaging

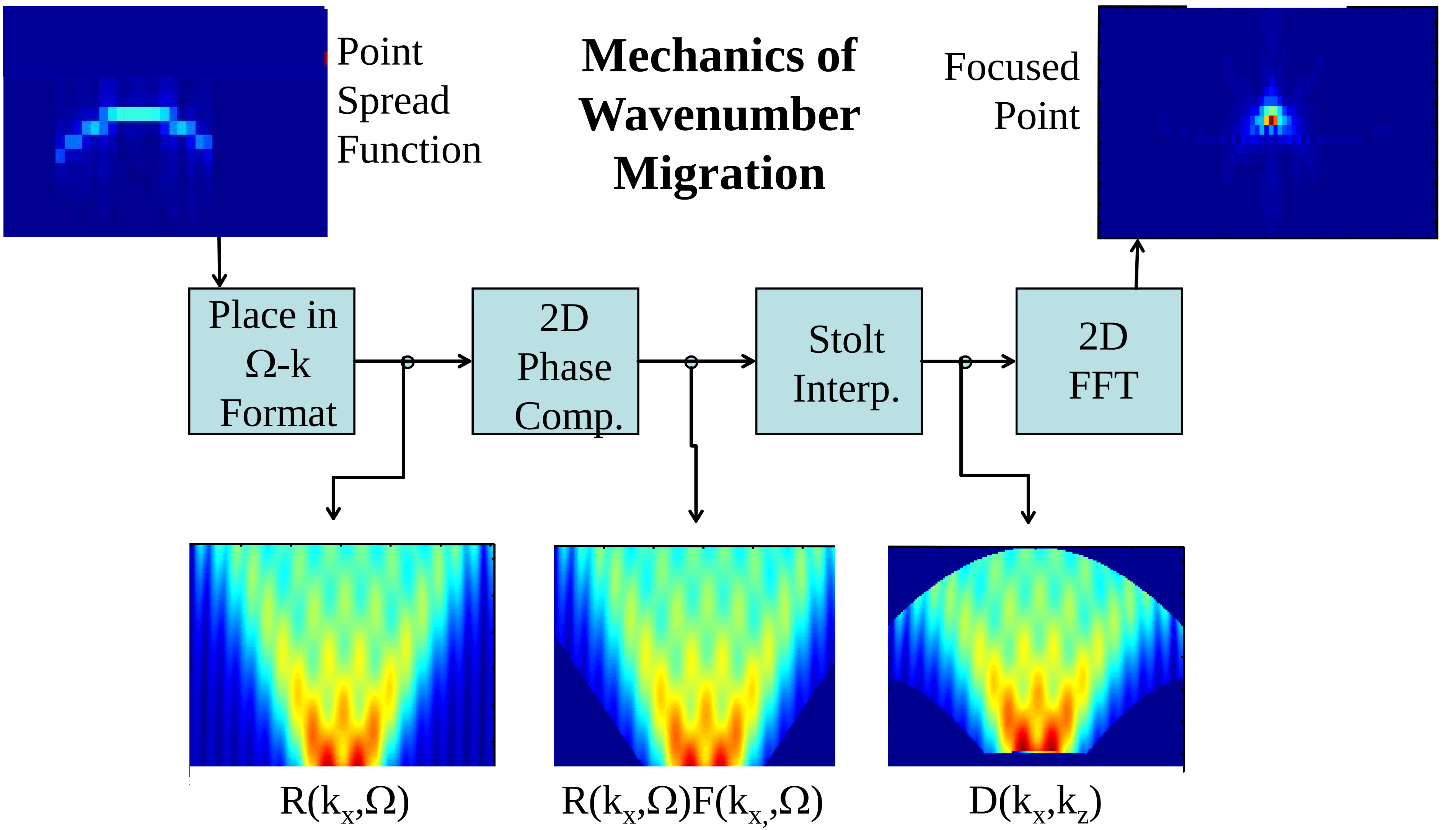
Point
Spread
Function
Mechanics of
Wavenumber
Migration
Focused
Point
Place in
Ω-k
Format
2D
Phase
Comp.
Stolt
Interp.
2D
FFT
$R(k_x,\Omega)$
$R(k_x,\Omega)F(k_x,\Omega)$
$D(k_x,k_z)$

Imaging

Matrix Implementation of Wavenumber Migration

Scene Grid

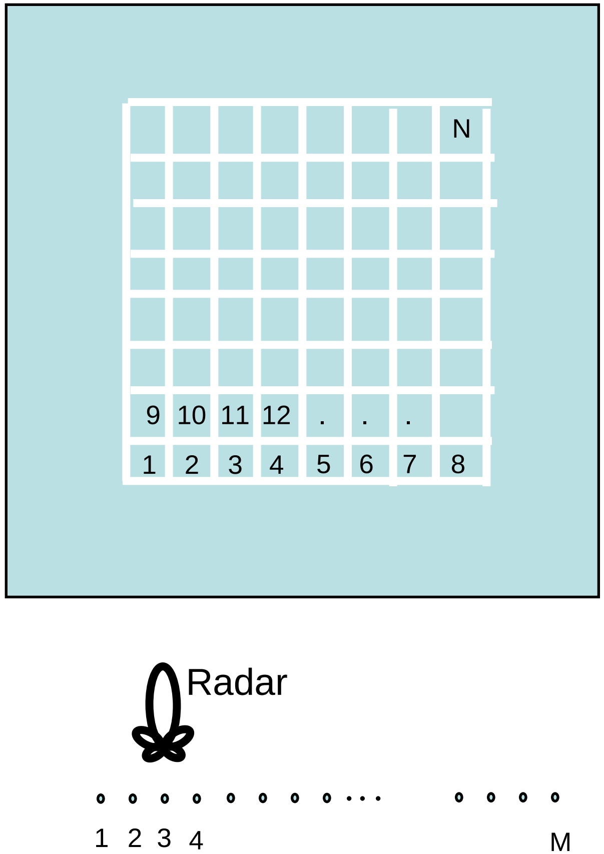

Observation Points in Regular Array

- Standard Wavenumber Migration

$$\underline{\hat{x}} = FFT^{-1}\left[f\left(FFT\left[\underline{y}\right]\right)\right]$$

$f\left(\underline{y}\right)$ – Modification to the observations

$$\underline{\hat{x}} = Q_2^{-1}\Phi Q_1 \underline{y}$$

$$\underline{\hat{x}} = FFT_2^{-1}\left[\Phi FFT_1\left[\underline{y}\right]\right]$$

- Φ is a Sparse Matrix – This allows for even faster computation.

Imaging

Sparse Reconstruction

- Radar imagery often has a significant number of zero pixels.

- We want to make use of this fact to produce better reconstructions.

- A Sparsity Model for an image is proposed as an exponential distribution of pixel amplitudes combined with a discrete probability of zero.

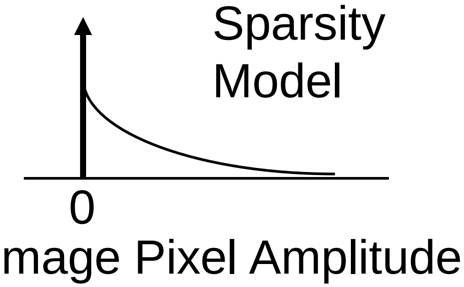

$$f_X(x) = (1-\omega)\delta(x) + \omega a e^{-a|x|}$$

- This sparsity constraint cannot be implemented like the standard Lagrange Multipliers.

Imaging

Making use of Sparsity

Original Signal Model: $$Y = HX + N$$

De-convolution and
De-noising Formulation

$$Y = HZ + N_1$$

$$Z = X + N_2$$

E step: $$\hat{Z}^{(n)} = \hat{X}^{(n)} + \alpha H^T (Y - H\hat{X}^{(n)})$$

Landweber Iterations

M step: $$\hat{X}^{(n+1)} = \arg\max \frac{\left\| \hat{Z}^{(n)} - X \right\|^2}{2\sigma_2^2} + p(X)$$

p(x) – A Penalty Term

Imaging

Implementing a Sparsity Constraint

M step: $$\hat{X}^{(n+1)} = \arg\max \frac{\left\| \hat{Z}^{(n)} - X \right\|^2}{2\sigma_2^2} + p(X)$$

Sparse Prior Information

Average Number of Zero Pixels
Statistical Distribution of Non-zero Pixels

Soft Thresholding Implementation*

M step: $$\hat{X}^{(n+1)} = \hat{Z}^{(n)}$$

*M. Figueiredo and R. Novak, "An EM Algorithm for Wavelet-based Image Restoration," IEEE Trans. Image Processing, vol. 12, pp. 906-916, 2003.

l_0 penalty function

Number of Non-zero pixels

l_1 penalty function

$$p(X) = \lambda \left| X \right|$$

M Step

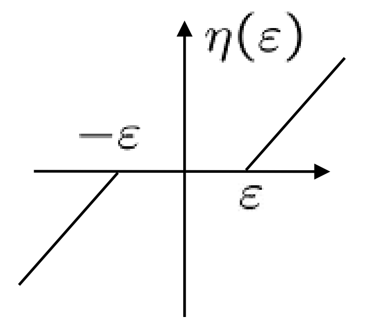

Pixel-wise
Soft Threshold
(Applied to Amplitude)

Imaging

Efficient Landweber Iterations

Imaging

Un-Imaging

$$\hat{Z}^{(n)} = \hat{X}^{(n)} + \alpha H^{T}\left(Y - H\hat{X}^{(n)}\right)$$

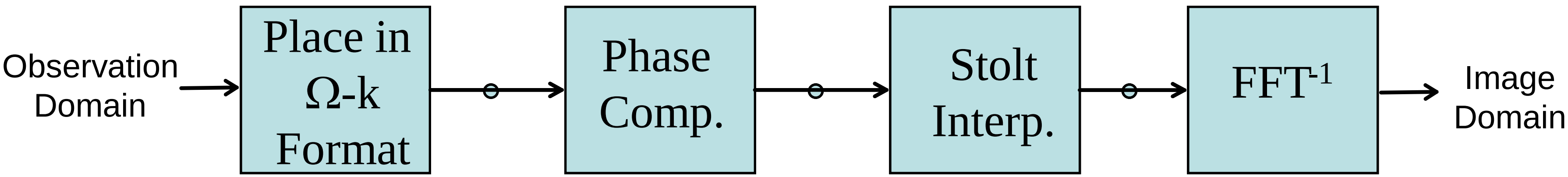

Forward Wavenumber Migration (Imaging)

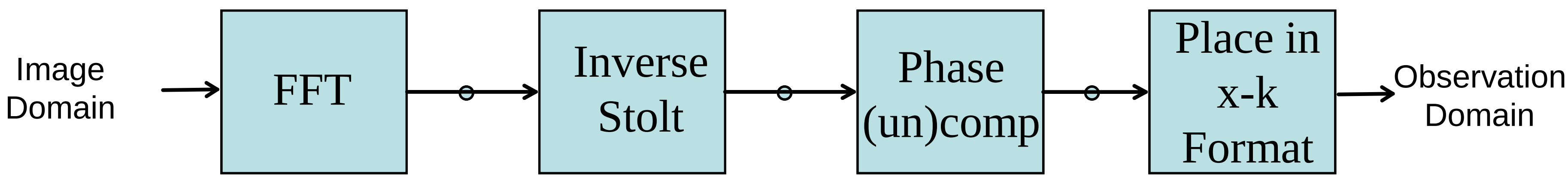

Reverse Wavenumber Migration (Un-imaging)

Imaging

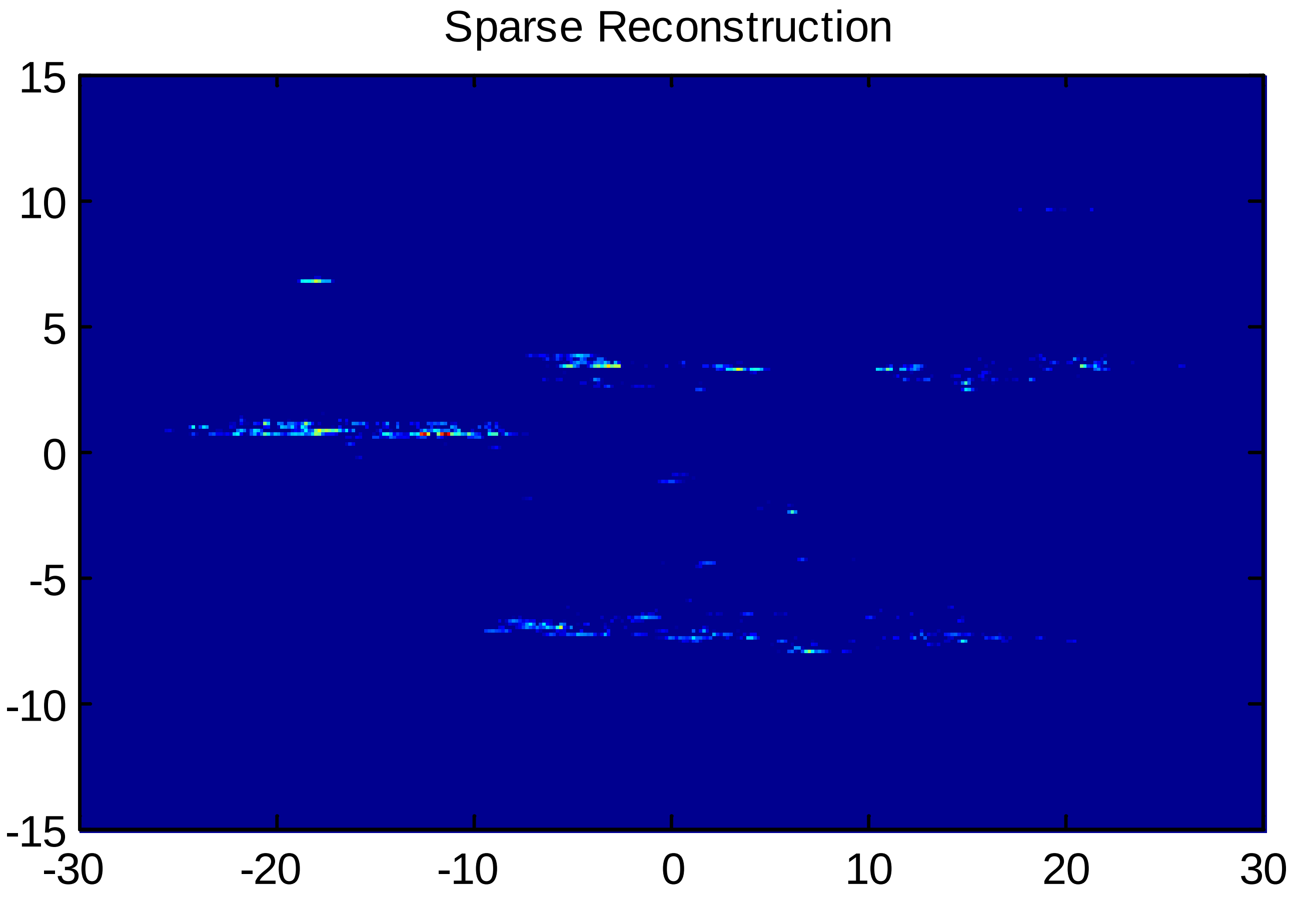

Imaging

3D Landmine Imaging

Want to determine:
- Object depth and size
- In Three Dimensions
- In Near Real Time

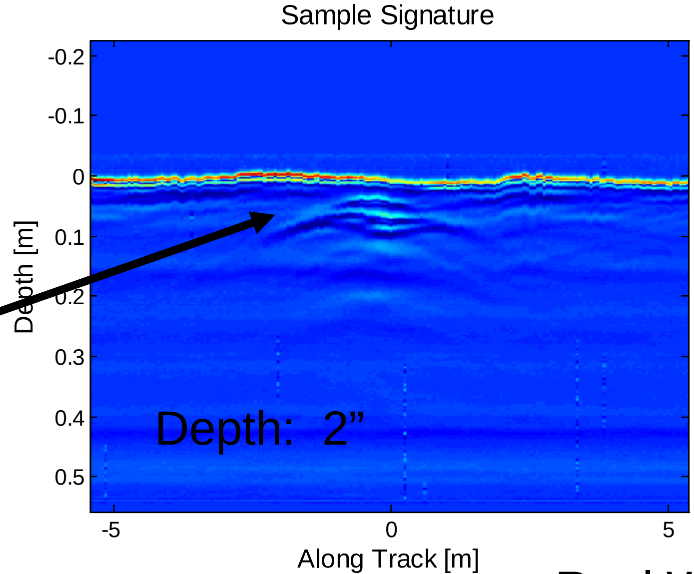

Real World Bounding Box

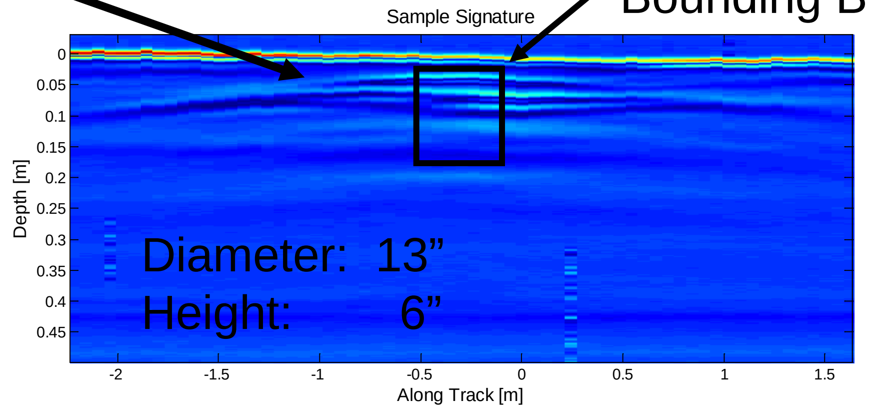

GPR Radar System

Imaging

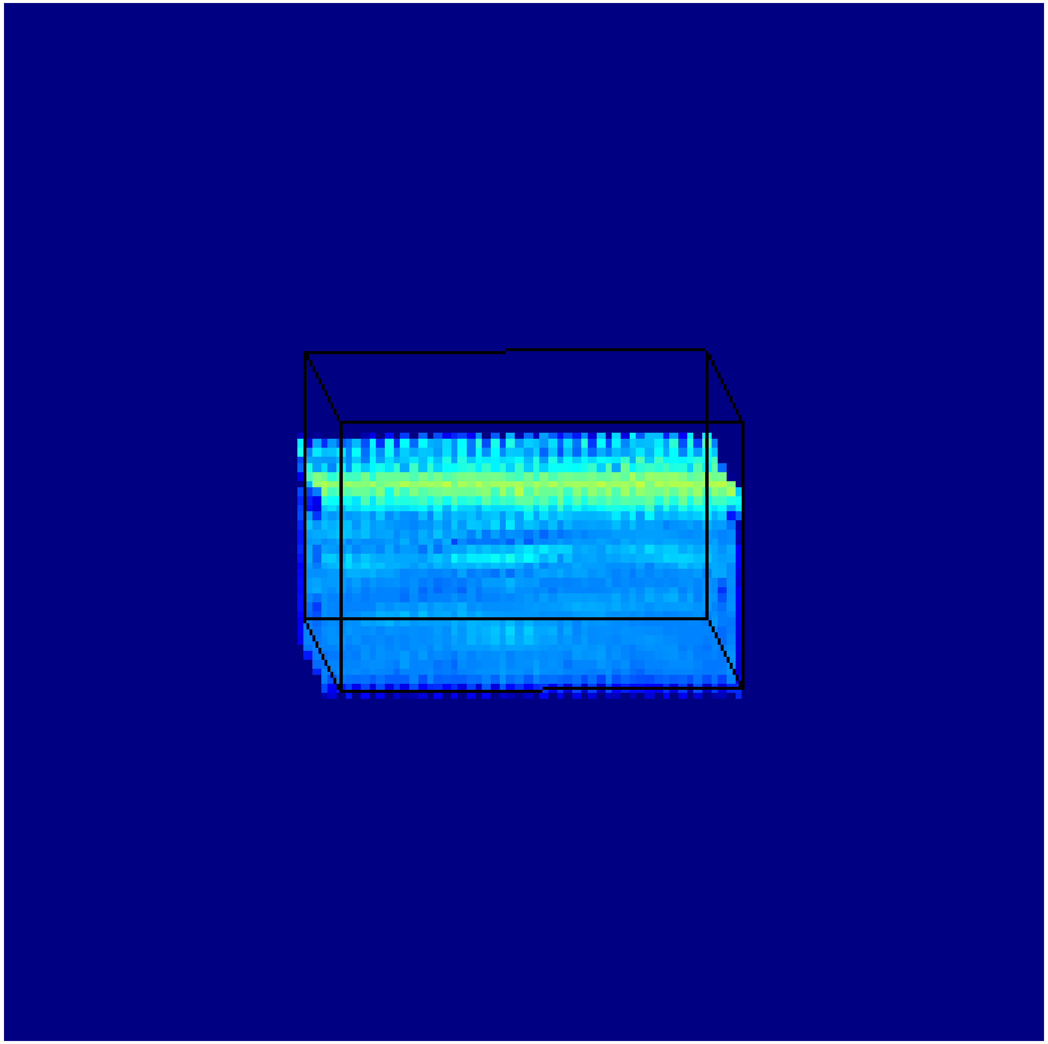

Raw GPR Data

Imaging

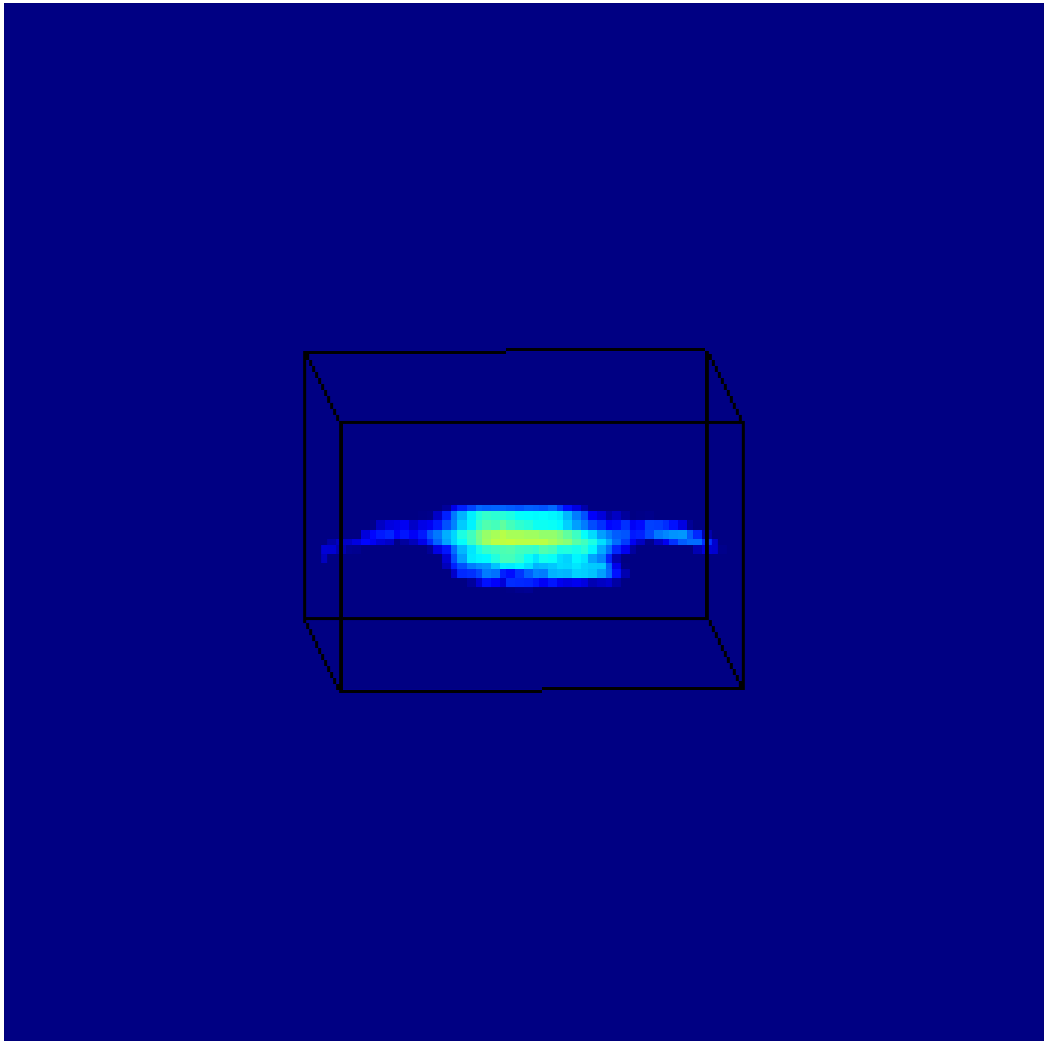

Wavenumber Migration

Imaging

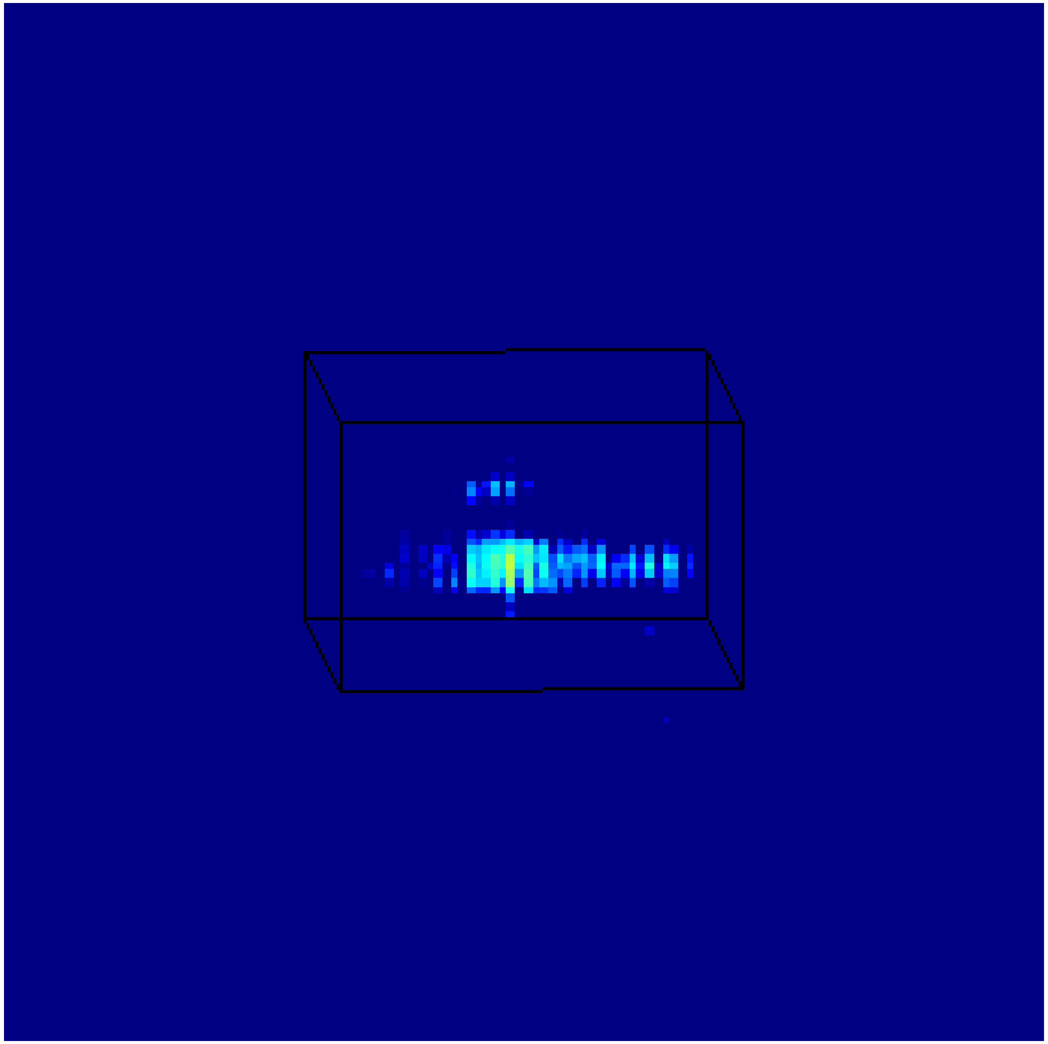

Sparse Reconstruction

Imaging Contributions

- Marble,J.A., Hero,A.O., ``Iterative Redeployment of Illuminatiion and Sensing (IRIS): Application to STW-SAR Imaging,'' in Proc. of the 25th Army Science Conference, Orlando, FL, Nov. 2006.

- Marble,J.A., Hero,A.O., ``Phase Distortion Correction for See-Through-The-Wall Imaging Radar,'' ICIP: International Conference on Image Processing 2006, Atlanta, GA, Oct. 2006.

- Marble,J., Hero,A, ``See Through The Wall Detection and Classification of Scattering Primitives,'' SPIE: Detection and Remediation Technologies for Mines and Minelike Targets XI, March 2006, Orlando, FL.

Conclusions

Major Contributions of this Thesis

- Landmine Detection/Classification
  - SNR enhancement of both GPR and EMI signals.
  - Sensor Scheduling of Confirmation Sensors
- I.R.I.S. Numerical Simulation
  - Iterative Redeployment of Imaging and Sensing
  - Adaptively build a large scene out of small aperture radar measurements.
  - Use sensor scheduling to redeploy small aperture radar.
- Fast Imaging of Large Scenes
  - 2D for STW and 3D for Landmine
  - Matrix Implementation of Wavenumber Migration
  - Fast Adjoint Operator based on “Reverse Wavenumber Migration”